



Account/Revue

# Phosphine supported metal-dihydrogen complexes: Elongation of H–H bond to reversible release of H<sub>2</sub>

Saikat Dutta

Department of Chemistry, North Campus, University of Delhi, Delhi 110007, India

## ARTICLE INFO

## Article history:

Received 23 January 2011

Accepted after revision 30 August 2011

## Keywords:

Phosphines  
Dihydrogen complexes  
Dihydrogen activation  
Elongated dihydrogen  
Dihydrogen release  
H-atom dynamics

## ABSTRACT

Monodentate and bidentate phosphine supported transition metal-dihydrogen complexes were studied extensively in last three decades by using spectroscopic (IR, NMR) and structural (X-ray and neutron single crystals diffraction) characterization techniques. A major concern was to investigate various changes in physical and chemical properties of H<sub>2</sub> when bound to a metal center. This article emphasizes the role of the electron rich phosphine ligands in forming molecular hydrogen complexes for a large number of transition metal ions and how the bonding of the metal with the molecular hydrogen (H<sub>2</sub>) affects the ultimate fate of the H–H bond. Important features of the H<sub>2</sub> complexes such as elongation of the H–H bond, rapid dynamics of the site exchange of H atoms in hydride/dihydrogen complexes, binding of H<sub>2</sub> to the coordinately unsaturated metal centers are discussed in great detail. In many cases, the results of spectroscopic and structural studies were supported by theoretical calculations. Besides these, the focus of the present article is on the phenomena of reversible release of H<sub>2</sub> observed in the case of certain recently reported metal-H<sub>2</sub> complexes which has relevance in H<sub>2</sub> production. Various features of the elongated H<sub>2</sub> complexes and reversible binding of H<sub>2</sub> to a metal center discussed in this article will be of great interest to inorganic and organometallic chemists in general and to inorganic-material chemists working in the area of catalysis and storage materials using H<sub>2</sub>. Discussions on certain new directions of metal-dihydrogen chemistry such as photochemical generation of H<sub>2</sub> complexes, ionic H<sub>2</sub> activation, and H<sub>2</sub> reductive elimination from polyhydride complexes have been included (202 references).

© 2011 Académie des sciences. Published by Elsevier Masson SAS. All rights reserved.

## 1. Abbreviations

Å	Angstrom
<sup>t</sup> Bu	<i>tert</i> -butyl
Cy	Cyclohexyl
DFT	Density functional theory
<i>d</i> <sub>HH</sub>	H–H bond distance
dppe	bis-diphenylphosphinoethane
dppm	bis-diphenylphosphinomethane
dmpe	bis-dimethylphosphinoethane
depe	bis-diethylphosphinoethane

dppip	2,2-bis(diphenylphosphino)propane
dmpm	bis-dimethylphosphinomethane
nod	Norboradiene
PES	Potential energy surface
Ph	Phenyl
<i>T</i> <sub>1</sub>	Spin-lattice relaxation time
triphos	MeC(CH <sub>2</sub> PPh <sub>2</sub> ) <sub>3</sub>

## 2. Introduction

Since the remarkable discovery of bonding of a nearly intact H<sub>2</sub> to metal center in sterically congested phosphine supported tungsten complexes [W(CO)<sub>3</sub>(PR<sub>3</sub>)<sub>2</sub>(H<sub>2</sub>)] (R = cyclohexyl **1** or isopropyl **2**) by Kubas and co-workers

Email address: saikatdutta2008@gmail.com.

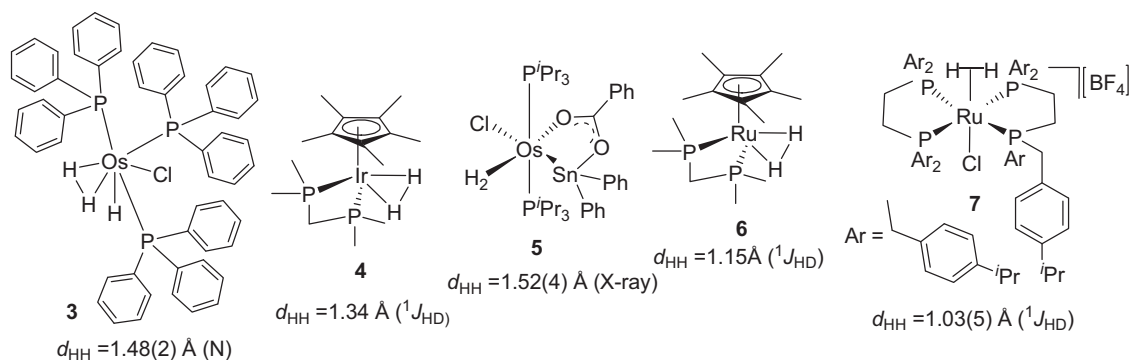


Fig. 1. Elongated  $H_2$  complexes with corresponding H–H distances.

in 1984 [1–4], a new area of research developed. Surprisingly, oxidative addition of metal bound  $H_2$  was inhibited in these complexes due to the suitable sterics and electronics. In last two decades, a large number of phosphine supported metal- $H_2$  complexes, their physical properties, and reactivities were reported by Morris, Crabtree, Chaudret and Heinekey and several reviews have been published [5–9]. A large number of these metal- $H_2$  complexes were characterized by several methods such as NMR spectroscopy, vibrational spectroscopy, X-ray and Neutron diffraction structure determination. The M- $H_2$  complexes are important for the chemical topologies and especially interesting for their unconventional structural features and dynamics of  $H_2$  bound to the metal center. Investigations on the structure and reactivity of the  $H_2$  complexes with elongated H...H moiety have been a challenging target in this area of research [8]. Elongated  $H_2$  complexes have been considered as the snapshots at various points of the oxidative addition of  $H_2$  to a metal center. In last two decades, various theoretical approaches [10–14] and numerous experimental findings [15–36] on structure and dynamics of the elongated  $H_2$  complexes in solution and solid state have been made. A list of metal- $H_2$  complexes and their H–H bond distances ( $d_{HH}$ ) are shown in Fig. 1.

Generally, transition metal polyhydride complexes exist in several nearly equivalent structures which demonstrates rapid permutation of the hydride positions often identified by variable temperature  $^1H$  NMR spectroscopy [37]. Polyhydride complexes contain a central metal with high coordination numbers (CN 7–9). In such cases, observed NMR parameters have been a population-weighted average of all the hydride environments. Dynamics of H-atom site exchange in polyhydrides have been rather complex, and a simplified version can be anticipated in the case of a *cis*-M(hydride/dihydrogen) structural arrangement in which rapid exchange of the H atoms between the metal bound hydride and dihydrogen site can be characterized and thermodynamic parameters can also be estimated. These complexes demonstrated a very rapid H atom exchange which leads to a single resonance corresponding to all the H nuclei. Consequently it is rather difficult to find out many important thermodynamic parameters of the process [38–56]. However, only for a limited number of cases molecular structures were confirmed by the spectroscopic methods in solution [42,43,45]. A series of *cis*-M(H)( $H_2$ ) complexes 8–14 supported by the ancillary ligands are shown in Fig. 2.

A coordinately unsaturated metal center favors a strong sigma donor-acceptor interaction with an unreactive

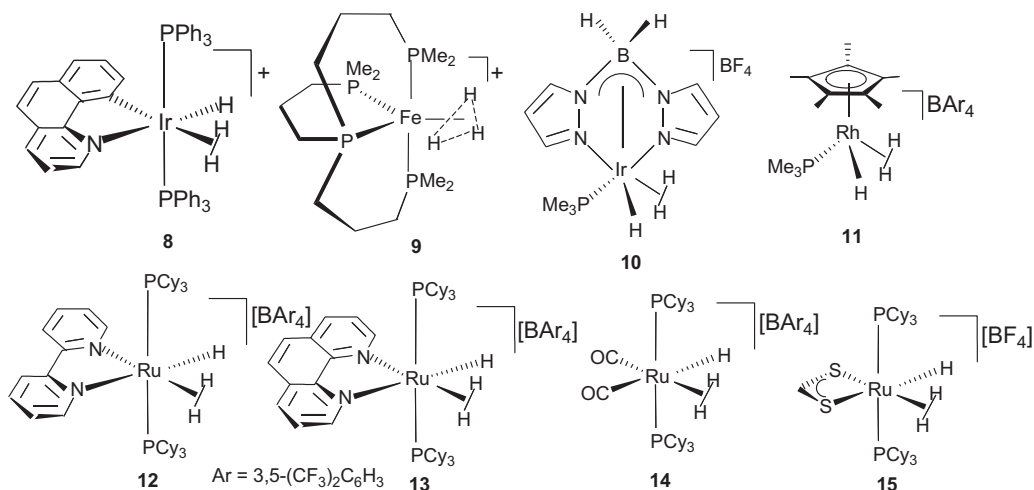


Fig. 2. *cis*-M(H)( $H_2$ ) complexes with rapid H-atom exchange.

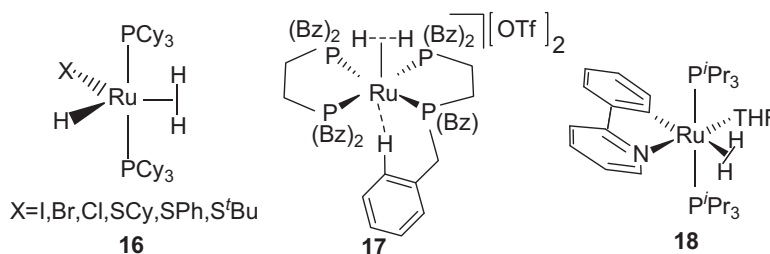


Fig. 3. Coordinately unsaturated H<sub>2</sub> complexes.

H–H sigma bond and a number of unprecedented complexes of similar properties are shown in Fig. 3. These complexes are often stabilized by intramolecular agostic interactions within the metal and H atom of the ancillary ligand which provides a considerable stability to M( $\eta^2$ -H<sub>2</sub>) moiety [57–61].

An extensive search for the alternative energy sources might stop at H<sub>2</sub> as cleavage of the H–H bond could meet the demand of the cleanest and safest energy. Reversible uptake of molecular hydrogen and efficient release for fueling under mild conditions have been among the major factors of the H<sub>2</sub>-storage applications [62–66]. In this direction, reversible releases of H<sub>2</sub> from certain transition metal complexes with phosphine ligands have been examined. Complexes with reversible H<sub>2</sub> binding capacity received much attention in the last decade and they are relevant for the study of biological H<sub>2</sub> production in nature [67–69].

### 3. Scope

Discussion in the present review will be restricted within only the phosphine containing transition metal molecular hydrogen (H<sub>2</sub>) complexes which are capable of H–H bond activation under mild conditions. A brief account on the recent advances in elongated dihydrogen complexes and the factors responsible for the elongation of H–H bond are discussed. It is beyond the scope of this review to give an in-depth analysis of transition metal dihydrogen complexes and their application in catalysis, however, this review is concerned with the structure and bonding of H<sub>2</sub> in phosphine supported dihydrogen complexes, elongated H<sub>2</sub> complexes for constructing the reaction coordinate of oxidative addition of H<sub>2</sub> in a metal center, and rapid H-atom site exchange phenomena in *cis*-dihydrogen-hydride complexes. The review begins with a brief description of the H<sub>2</sub> activation, related features and effect of the coordination of the phosphines on the H–H distances. A considerable number of elongated dihydrogen complexes have been systematically studied in the recent years and it seemed suitable to describe the essential features of some of these compounds especially the H...H elongation and its temperature dependence. However, readers should be able to access a selection from the cited appropriate references. The phenomena of reversible release of H<sub>2</sub> with a series of recently developed dihydrogen complexes are included. This indeed gives a scope to relate the topics discussed herein with the research on the H<sub>2</sub> as the alternative source of energy. The

aim is to provide the readers with an appreciation for further progression of this field and insight of the aspects on which metal-H<sub>2</sub> chemistry should be studied.

## 4. Phosphine supported metal-H<sub>2</sub> complexes

### 4.1. Discovery of dihydrogen complex

A strong H–H sigma bond (435 kJ mol<sup>-1</sup>) [70] makes molecular hydrogen extremely inert to break apart H atoms and it is chemically useful only when a controlled bond cleavage process occurs. It is important to know the process of H<sub>2</sub> activation (bond cleavage) either via a chemical method (metal complexes) or by enzymes (hydrogenase). The mechanism of H–H bond splitting was not fully understood until the discovery of Kubas and co-workers on the coordination of an intact H<sub>2</sub> molecule to a metal complex in 1984 which ultimately catalyzed a new area of research to develop [1–3]. The H<sub>2</sub> binds in a side-on fashion to the metal center by  $\sigma$  electron donation and molecules containing such non-classical 2-electron 3-center bond termed as the “ $\sigma$  complex” [40]. Oxidative addition of H<sub>2</sub> to a metal center and the formation of the metal dihydride are well-established phenomena in homogeneous hydrogenation processes. Apart from the oxidative addition, reversible binding of H<sub>2</sub> was also observed for coordinately unsaturated 16-electron complexes such as M(CO)<sub>3</sub>((PCy<sub>3</sub>)<sub>2</sub>) (M = W **1**, Mo **2**, Cy = cyclohexyl) [71] in which a phosphine CH is weakly interacting with the sixth coordination site via an agostic interaction. Such electronic unsaturation in these complexes is responsible for the reversible binding of H<sub>2</sub> at ambient conditions [72]. Sterically congested phosphines such as PR<sub>3</sub> (R = cyclohexyl, isopropyl) played a crucial role in inhibiting the oxidative addition of metal bound H<sub>2</sub> which results metal-dihydride species. There are several examples of elongated metal-H<sub>2</sub> complexes exhibiting bonding with nearly intact H<sub>2</sub> and identified by their characteristic short <sup>1</sup>H spin-lattice relaxation times (*T*<sub>1</sub> < 100 ms) [73].

### 4.2. Metal-phosphine coordination

Phosphines are one of the important families of ligand in both academic and industrial spheres. Neutral and electron donor phosphine usually binds to a transition metal through their phosphorous lone pairs. Commonly used in dihydrogen chemistry are monodentate (PR<sub>3</sub>) and bidentate (R<sub>2</sub>P(CH)<sub>*n*</sub>PR<sub>2</sub>) (R = alkyl, aryl, *n* = 1, 2, 3)

phosphines. Phosphines have been ubiquitous as ancillary ligands in transition metal chemistry and homogeneous catalysis. Phosphine supported dihydrogen complexes have been found to be efficient for many catalytic processes such as transfer hydrogenation [41,74–96], isotope exchange [97–102], hydrosilylation [89,103–106], C–C coupling [107–109] involving the cleavage of H–H bond. Use of the monodentate and bidentate phosphines enforces the required electronic effect on the metal center through its sigma ( $\sigma$ ) donor ability to an empty orbital of the metal and the back donation component from a filled orbital of the metal to P–R antibonding ( $\sigma^*$ ) orbital. Phosphines can also exhibit a range of sigma donor and pi-acceptor abilities when electron-withdrawing (electronegative) to electron donating substituents are attached to the donor phosphorous atoms. This gives the scope to fine tune the electronic properties of the metal complexes by varying the substituents with different electron donor or accepting ability. The fine-tuning of the metal center is essential for dihydrogen complexes in order to improve stability and reactivity. For such variations, phosphines are the ideal candidate as ancillary ligands in the chemistry of metal-H<sub>2</sub> complexes. The effect of the phosphines binding to a metal center is pictorially represented with a simplified molecular orbital diagram in Fig. 4.

To examine the bonding features of the M( $\eta^2$ -H<sub>2</sub>) moiety and the H–H distance upon bound to the metal, it is very important to fine tune and manipulate the electron density on the metal center. An ordering of the sigma-donating and pi-accepting abilities of the phosphine ligands can be utilized to construct a series of dihydrogen

complexes with only difference in structural features of the phosphine (sterics and electronics) which would dictate the fate of the bonding of H<sub>2</sub>. By the effective fine-tuning of electronics and sterics of phosphine, one can construct a series of dihydrogen complexes of variable H–H distances along the reaction coordinate for the oxidative addition (OA) of H<sub>2</sub>. In case of the Kubas's systems [W(CO)<sub>3</sub>(PR<sub>3</sub>)( $\eta^2$ -H<sub>2</sub>)] (R = Cy **1**, <sup>i</sup>Pr **2**), the side on bonding of H<sub>2</sub> was controlled by the electron donor ability of the phosphine and an equilibrium existed between dihydrogen and dihydride forms [1,3]. Snapshots of the different states of the oxidative addition of H<sub>2</sub> to a metal center were observed in a series of osmium complexes *trans*-[Os(R<sub>2</sub>PCH<sub>2</sub>CH<sub>2</sub>PR<sub>2</sub>)<sub>2</sub>(H<sub>2</sub>)(Cl)]<sup>+</sup> for which H–H distance increased upon increasing the electron donor ability of the phosphines with various R (Ph, Et and Cy) substituents [110]. Due to the chelation properties and high electron donor ability of the alkyl substituted bisphosphines, the amount of electron population on the  $\sigma^*$  orbital of H<sub>2</sub> was increased (Fig. 4). This led to a considerable elongation of the H–H bond, a very important process of interest.

#### 4.3. Homolytic and heterolytic activation of H<sub>2</sub>

The activation of H<sub>2</sub> on the metal center of  $\sigma$ -complexes undergoes *via* two different pathways, homolytic cleavage (oxidative addition) and heterolytic cleavage (deprotonation). Homolytic cleavage consists in the formation of a  $\sigma$ -complex which turns to metal dihydride by complete rupture of the H–H bond resulting an increase of the formal oxidation state of the metal by +2 (Scheme 1).

For the oxidative addition, the electronic factor on the metal is very important where the back donation of electrons from the metal to the  $\sigma^*$  orbital of the H<sub>2</sub> is crucial in stabilizing the  $\sigma$ -bonding and homolysis. Extensive efforts have been aimed at studying the stretching of the H–H bond toward oxidative addition by varying the electronics and sterics on the metal using different ancillary ligands. A large regiment of the M–H<sub>2</sub> complexes with a wide range of H–H distances varied from ( $d_{\text{HH}}$ ) 0.82 to 1.5 Å exhibited the stretching of the H–H bond ( $d_{\text{HH}}$ (gaseous H<sub>2</sub>) = 0.74 Å) [70] in different extents [15,110–114]. The reaction coordinate for the activation of H<sub>2</sub> on a metal center with corresponding H–H distances ( $d_{\text{HH}}$ ) is represented in Scheme 2 [115]. Note that *elongated* H<sub>2</sub> complexes ( $d_{\text{HH}}$  = 1–1.3 Å) and compressed dihydrides ( $d_{\text{HH}}$  > 1.3 Å) are two different classes of compounds possessing significantly contrasting structural features and physical properties in solution.

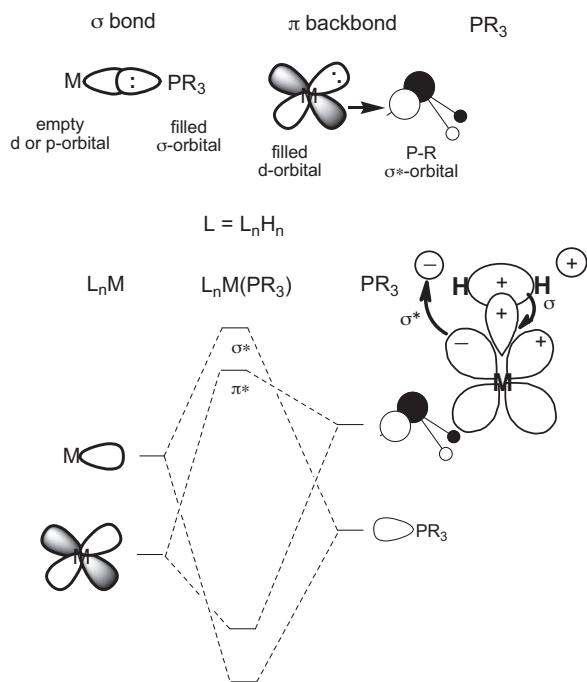
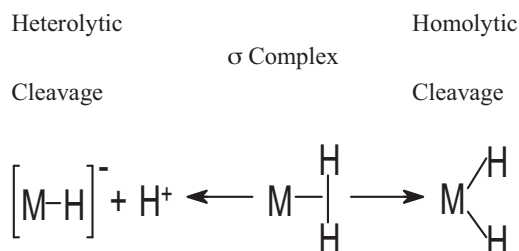
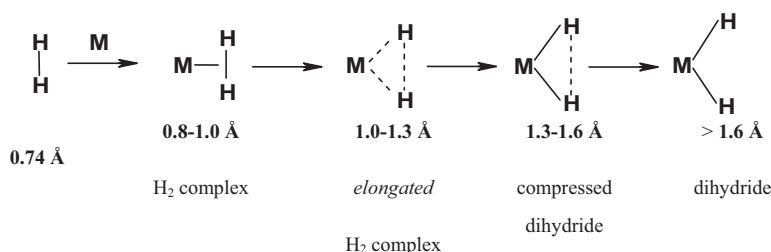


Fig. 4. Simplified molecular orbital diagram of a phosphine supported metal-dihydrogen complex.



Scheme 1. Heterolytic and homolytic cleavage of H<sub>2</sub> on a metal center.



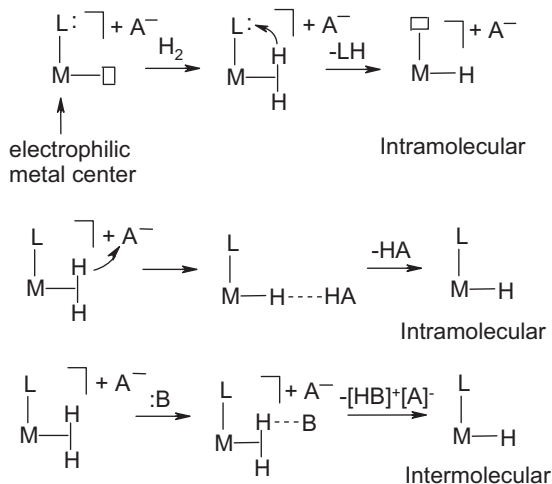
Scheme 2. Different stages of H–H bond cleavage on a metal center [114].

Heterolytic activation of  $H_2$  wherein H–H bond is cleaved into  $H^+$  and  $H^-$  fragments is now considered. In this process, neither the metal oxidation state nor the coordination number changes. The metal center is generally electrophilic when containing ligands with strong  $\pi$ -acceptors properties such as CO particularly when trans to  $H_2$  in the case of  $[Re(H_2)(CO)_4(PPh_3)]$  **19** [116] or in case of the highly cationic complex such as *trans*- $[Os(CH_3CN)(H_2)(dppe)]^{2+}$  **20** [117]. There are general pathways for the heterolytic cleavage of the  $H_2$  on the metal center. It was observed that addition of gaseous  $H_2$  to unsaturated precursors or by protonation of a M–H bond from which a proton can split out and either migrate to an external Lewis base (intermolecular) or be directly transferred to a coligand or anion (intramolecular) (Scheme 3) [118].

In electrophilic cationic metal complexes, metal bound  $H_2$  is highly acidic and polarized to  $H^{\delta+}-H^{\delta-}$  species from which ready transfer of  $H^+$  is facile. In such systems,  $pK_a(H_2)$  becomes low as  $-2$  to  $-5$  which was determined by measuring concentrations of different species present in equilibrium by  $^1H$  NMR spectroscopy [111,118,119]. This makes  $\eta^2-H_2$  a strong acid and acidity of the  $H_2$  complex goes high [111,120]. Intramolecular heterolysis involves proton transfer to the *cis* ligand L or to the counterion  $A^-$  of a cationic complex in which most of the L ligands were highly basic such as an amine [121] or thiolate [122] which facilitate the reaction. Intermolecular base assisted

heterolysis and protonation of an external base gives metal hydride and the conjugate acid of the base  $HB^+$ . The reactions depicted in Scheme 3 were reversible as described by DuBois and coworkers; heterolytic cleavage of the  $H_2$  should be at or near equilibrium to avoid high-energy intermediates [123,124].

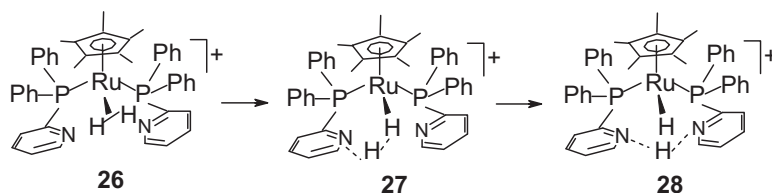
However, there are only limited cases where electron donor phosphine supported  $H_2$  complexes undergo heterolysis of  $H_2$ . A highly electrophilic coordinately unsaturated 16 electron complex  $[Ru(P(OMe)(OH)_2)(dppe)_2]^{2+}$  **21** turned  $H_2$  gas into a strong acid by heterolytic activation [125]. Similarly, a metallo-phosphorous acid derivative  $[Ru(P(OH)_3)(dppe)_2]^{2+}$  **22** was strongly electrophilic for heterolysis of  $H_2$ . It was observed that the complex  $[Ru(P(OMe)(OH)_2)(dppe)_2]^{2+}$  **21** reacts with  $H_2$  (as head gas) in  $CD_2Cl_2$  at 273 K which resulted a hydride derivative *trans*- $[Ru(H)(P(OMe)(OH)_2)(dppe)_2]^+$  **23**. This process of heterolysis was suppressed in the presence of HOTf [125]. Generation of HOTf and *trans*- $[Ru(H)(P(OH)_3)(dppe)_2]^+$  **24** in this process supports that the reaction proceeds via the intermediacy of a dicationic dihydrogen complex, *trans*- $[Ru(\eta^2-H_2)(P(OH)_3)(dppe)_2][OTf]_2$  **25**. The HD derivative of complex **25** exhibited a 1:1:1 triplet with a  $^1J_{HD}$  of 33.3 Hz which corresponds to a H–H distance 0.86 Å using the Morris relation [110,125]. The positive charge on the metal and the electron-withdrawing nature of coligand *trans* to the  $H_2$ , significantly increased the acidity resulting heterolytic splitting of  $H_2$ . Another case of heterolysis of  $H_2$  was reported by Chin et al. in which case a mild base  $NEt_3$  assisted the deprotonation of the  $\eta^2-H_2$  tautomer in the equilibrium mixture of  $\eta^2-H_2/(H_2)$  (84:16) as shown in Eq. (1) [127].

Scheme 3. Heterolytic cleavages of  $H_2$  [117].

Probably even more importantly, heterolytic activation of  $H_2$  is interesting where it is applicable for reactions like ionic hydrogenation of unsaturated bonds using a metal catalyst [87]. A case of the intramolecular proton transfer assisted  $H_2$  heterolysis was found for complex **26** supported by a phosphinopyridine ligand (Scheme 4) [128]. Apart from these, there are only a limited number of phosphine supported metal complexes of Ru and Os in which  $H_2$  ligand undergoes heterolytic splitting due to the electrophilicity of the metal [116,129,130].

Heterolytic splitting of  $H_2$  was also found relevant in catalytic processes such as hydrogenation of alkynes and ketones in which heterolysis of  $H_2$  was involved in the key





Scheme 4. Intramolecular proton transfer and H<sub>2</sub> heterolysis on Ru complex [127].

steps [130,131]. Generally, it is observed that an acidic H<sub>2</sub> complex is involved in the proton-transfer step in catalysis via heterolytic splitting [132]. Intramolecular heterolysis of H<sub>2</sub> is the most essential step in many diverse systems including metalloenzymes such as hydrogenases [117,133]. Hydrodesulfurization (HDS) is also among the processes in which heterolytic splitting of H<sub>2</sub> being obvious in heterogeneous phase for metal sulfides (MoS<sub>2</sub> and RuS<sub>2</sub>) [134,135].

## 5. Activation of H<sub>2</sub> in transition metal complexes

### 5.1. Periodic trend

A large number of H<sub>2</sub> complexes were reported in the last 25 years of research by many researchers. Among these, a large number of neutral and cationic H<sub>2</sub> complexes were stabilized by the electron donor phosphines. A brief account of H<sub>2</sub> complexes of different group elements would give an idea of the nature of the compounds. Generally, transition metals from vanadium to platinum form dihydrogen complexes of which some are thermally unstable, transient species, and rest of the complexes are stable in solution for a limited period. Only a limited number of complexes are found to be stable in the solid state. A literature study reveals there are no examples of H<sub>2</sub> complexes of early transition metals, so also no report yet on the stable dihydrogen complex of lanthanides and actinides [136].

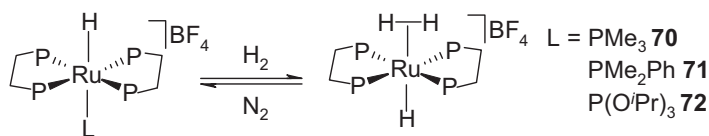
Vanadium which forms stable H<sub>2</sub> complexes at sufficiently low-temperature with a dihydrogen/dihydride interconversion and a similar behaviour was observed for the Nd and Ta derivatives as well [137]. Group 6 transition metals form H<sub>2</sub> complexes of which a series of chromium complexes Cr(CO)<sub>3</sub>(PR<sub>3</sub>)<sub>2</sub>(H<sub>2</sub>) (R = Cy **29**, <sup>i</sup>Pr **30**) was structurally characterized using X-ray crystallography and inelastic neutron scattering spectroscopy [138]. In another study, an equilibrium dissociation of the H–H bond was reported for a series of Mo complexes Mo(CO)<sub>3</sub>(PR<sub>3</sub>)<sub>2</sub>(H<sub>2</sub>) (R<sub>3</sub> = Cy<sub>3</sub> **31**, *i*-Pr<sub>3</sub> **32**, Cy<sub>2</sub>-*i*-Pr **33**) resulting in 7-coordinated dihydrides MH<sub>2</sub>(CO)<sub>3</sub>(PR<sub>3</sub>)<sub>2</sub> which exist with a dihydrogen-hydride equilibrium. The interconversion feature in these complexes is controlled by the sterics of the substituents of the phosphine [2].

Implications on the reaction coordinate for the oxidative addition of H<sub>2</sub> to a metal center is one of the major concerns of transitional metal-H<sub>2</sub> chemistry. Toward this direction a series of complexes Mo(CO)(R<sub>2</sub>PCH<sub>2</sub>CH<sub>2</sub>PR<sub>2</sub>)<sub>2</sub> (R = Et **34**, <sup>i</sup>Bu **35**, Ph **36**, Et-Ph **37**) supported by the bisphosphine ligands, was examined. In this study, complexes **34** and **35** showed oxidative addition of H<sub>2</sub> resulting Mo-dihydrides whereas

formation of a stable M(η<sup>2</sup>-H<sub>2</sub>) form was confirmed for the complex **36** [139]. Further studies on the interplay of η<sup>2</sup>-H<sub>2</sub> versus dihydride form for a series of complexes Mo(H<sub>2</sub>)(-CO)((RCH<sub>2</sub>)<sub>2</sub>PCH<sub>2</sub>CH<sub>2</sub>P(CH<sub>2</sub>R)<sub>2</sub>)<sub>2</sub> (R = Me **38**, Pr<sup>*i*</sup> **39**, C<sub>6</sub>H<sub>4</sub>X, X = H **40a**, *p*-Me **40b**, *m*-Me **40c**, *p*-OMe **40d**) gave the implications on the reaction coordinate for the homolysis of H<sub>2</sub>. In this case, when the dihydride formulation in Mo(H<sub>2</sub>)<sub>2</sub>(CO)(RCH<sub>2</sub>)<sub>2</sub>PCH<sub>2</sub>CH<sub>2</sub>(CH<sub>2</sub>R)<sub>2</sub> (R = Me **38**, Pr<sup>*i*</sup> **39**) was appropriate, the η<sup>2</sup>-H<sub>2</sub> coordination in *trans*-[Mo(H<sub>2</sub>)(-CO)((RCH<sub>2</sub>)<sub>2</sub>PCH<sub>2</sub>CH<sub>2</sub>P(CH<sub>2</sub>R)<sub>2</sub>)<sub>2</sub>] (R = C<sub>6</sub>H<sub>5</sub> **40a**, C<sub>6</sub>H<sub>4</sub>-*m*-Me **40c**) was established by structural and spectroscopic analysis [140]. These studies show the stabilization of a η<sup>2</sup>-H<sub>2</sub> is favored when the R is a poor electron donor, whereas a dihydride form is obvious when R is a highly electron donating such as alkyl. In another investigation with a solution of complex [Mo((NPh)(PMe<sub>3</sub>)<sub>2</sub>(*o*-(Me<sub>3</sub>SiN)<sub>2</sub>C<sub>6</sub>H<sub>4</sub>))] **41** under H<sub>2</sub> resulted in formation of [Mo(NPh)(PMe<sub>3</sub>)<sub>2</sub>(H<sub>2</sub>)(*o*-(Me<sub>3</sub>SiN)<sub>2</sub>C<sub>6</sub>H<sub>4</sub>)] **42** [141].

There were reports of only limited numbers of dihydrogen complexes of Mn, Tc, and Re metals in literature. A polyagostic 16-electron complex [Mn(CO)(-depe)<sub>2</sub>][BAR'<sub>4</sub>] (Ar' = C<sub>6</sub>H<sub>3</sub>(3,5-CF<sub>3</sub>)<sub>2</sub> **31**) forms a *trans*-[Mn(η<sup>2</sup>-H<sub>2</sub>)(CO)(depe)<sub>2</sub>][BAR'<sub>4</sub>] **43** when treated with H<sub>2</sub> [142]. Synthesis of the first η<sup>2</sup>-H<sub>2</sub> complex of technetium was reported wherein a 16-electron species [TcCl(dppe)<sub>2</sub>] **44** upon treated with H<sub>2</sub> resulted a dihydrogen complex which lose H<sub>2</sub> upon degassing the solution [143]. Cationic H<sub>2</sub> complexes [Re(H<sub>2</sub>)(PR<sub>3</sub>)<sub>2</sub>(CO)<sub>3</sub>][BAR'<sub>4</sub>] (PR<sub>3</sub> = PCy<sub>3</sub> **45**, P<sup>*i*</sup>Pr<sub>3</sub> **35**, P<sup>*i*</sup>PrPh<sub>2</sub> **46**, PPh<sub>3</sub> **47**; Ar' = 3,5-(CF<sub>3</sub>)<sub>2</sub>C<sub>6</sub>H<sub>3</sub>) of rhenium were susceptible to the heterolysis of H<sub>2</sub> which resulted in the lose of H<sub>2</sub> under vacuum and argon by resulting 16-electron species [144]. For another series of rhenium complexes Re(CO)(H<sub>2</sub>)L<sub>2</sub>(NO) (L = PCy<sub>3</sub> **48**, P<sup>*i*</sup>Pr<sub>3</sub> **49**, PMe<sub>3</sub> **50**, P(O<sup>*i*</sup>Pr)<sub>3</sub> **51**) [145] π-acid ligand *trans* to the metal-H<sub>2</sub> unit exhibited a highly acidic nature but stable toward the H<sub>2</sub> lose under positive pressure of H<sub>2</sub>.

In more recent studies on H<sub>2</sub> complexes, stereoelectronic parameters of a series of phosphorous ligands were determined by Woska et al. which revealed that PF<sub>3</sub> is the weakest σ-donor and the strongest π-acceptor as ancillary ligand [146]. During the same period, large numbers of ruthenium-H<sub>2</sub> complexes were reported and the influence of the ancillary ligands on the stability of H<sub>2</sub> was examined. Single crystal X-ray and neutron diffraction studies of *trans*-[Fe(η<sup>2</sup>-H<sub>2</sub>)(H)(Ph<sub>2</sub>PCH<sub>2</sub>CH<sub>2</sub>PPh<sub>2</sub>)<sub>2</sub>][BPh<sub>4</sub>] **52** by Morris and co-workers showed a H–H distance 0.816(16) Å [147]. In another study, the high acidity of the structurally similar complex *trans*-[Ru(η<sup>2</sup>-H<sub>2</sub>)(H)(R<sub>2</sub>PCH<sub>2</sub>CH<sub>2</sub>PR<sub>2</sub>)<sub>2</sub>]<sup>+</sup> was found to be variable with the electron donor ability of the chelating bis-phosphines. Further studies showed



Scheme 5. Facile formation of the trans hydride-dihydrogen complex  $\text{trans-}[\text{Ru}(\text{dppe})_2(\text{H})(\eta^2\text{-H}_2)][\text{BF}_4]$  in solution [155].

that upon increasing the electron donor ability of the phosphine by  $\text{R} = p\text{-CF}_3\text{C}_6\text{H}_4$  **53** to  $p\text{-MeOC}_6\text{H}_4$  **54**, the  $\text{pK}_a$  of the  $\text{H}_2$  complexes increased from 9 to 16 with a small change in the H–H distances [148].

Similarly, complexes  $\text{trans-}[\text{Ru}(\text{H}_2)(\text{Cl})(\text{dppe})_2]^+$  **55** and  $\text{trans-}[\text{Ru}(\text{H}_2)(\text{Cl})(\text{depe})_2]^+$  **56** showed the electron donor ability of the Cl and hydride *trans* to  $\eta^2\text{-H}_2$  influence the spin-lattice relaxation time ( $T_1$ , ms) and  $^1J_{\text{HD}}$  of  $\eta^2\text{-H}_2$  which resulted longer H–H distances for the Cl complex due to the enhanced  $d\pi(\text{Ru})\text{-}\sigma^*(\text{H}_2)$  back-donation. Surprisingly, the  $\text{trans-}[\text{Ru}(\eta^2\text{-H}_2)(\text{Cl})(\text{dppe})_2]^+$  **55** was sufficiently acidic as it reacted with the  $\text{H}_2$  and eliminated HCl to yield  $\text{trans-}[\text{Ru}(\eta^2\text{-H}_2)(\text{H})(\text{dppe})_2]^+$  **57** [149]. Monohydride complex  $[\text{RuH}(\text{dippe})_2]^+$  **58**, upon reacting with alkyne, yielded alkynyl- $\text{H}_2$  complexes  $[\text{Ru}(\eta^2\text{-H}_2)(\text{C}\equiv\text{CR})(\text{dippe})_2]^+$  [ $\text{R} = \text{Ph}$  **59** or  $\text{CO}_2\text{Me}$  **60**] (*dippe* = 1,2-bis(diisopropylphosphino)ethane) structurally determined by the X-ray crystallography [150].

Ruthenium dihydrogen complex  $\text{cis-}[\text{Ru}(\eta^2\text{-H}_2)(\text{H})(\text{diphosphine})_2]^+$  **61** (*diphosphine* = homoxantphos) with a wide bite angled chelating phosphine demonstrated the rapid H-atom exchange between the  $\eta^2\text{-H}_2$  and terminal hydride. The above-described complexes were thermally unstable toward hydrogen loss [151]. The evidence of turning the dihydrogen gas into a strong acid was reported for a  $\text{H}_2$  complex  $\text{trans-}[\text{Ru}(\eta^2\text{-H}_2)(\text{CNH})(\text{Ph}_2\text{P}(\text{CH}_2)_n\text{PPh}_2)_2][\text{O}_3\text{SCF}_3]_2$  ( $n = 2$  **62** or  $3$  **63**) [152]. Protonation of the hydride such as  $\text{CpRu}(\text{CO})(\text{PR}_3)\text{H}$  ( $\text{PR}_3 = \text{PPh}_3$  **64**,  $\text{PMe}_3$  **65**,  $\text{PMe}_2\text{Ph}$  **66**,  $\text{PCy}_3$  **67**) resulted in cationic  $\text{H}_2$  complexes  $[\text{CpRu}(\text{CO})(\text{PR}_3)(\eta^2\text{-H}_2)][\text{BF}_4]$  at  $-78^\circ\text{C}$  [132].

In a more recent study, an interesting observation was noted for a series of dicationic dihydrogen complexes  $\text{trans-}[\text{Ru}(\text{dppe})_2(\eta^2\text{-H}_2)(\text{L})][\text{BF}_4]_2$  (*dppe* =  $\text{Ph}_2\text{PCH}_2\text{CH}_2\text{PPh}_2$ ;  $\text{L} = \text{PF}(\text{OMe})_2$  **68**,  $\text{PF}(\text{OEt})_2$  **69**,  $\text{PF}(\text{O'Pr})_2$  **70**) in which influence of the cone angles [153] and the  $\pi$ -acceptor properties of phosphines played a major role [154]. The  $\text{H}_2$  nuclei, while bound to the metal, showed spin-spin coupling  $J(\text{H}, \text{P}_{\text{trans}})$  ranging from 49.5 to 50.4 Hz with the *trans* phosphorous moiety. Such large  $J_{\text{H}, \text{P}_{\text{trans}}}$  was also reported for a structurally similar complex  $\text{trans-}[\text{Ru}(\text{dppe})_2(\eta^2\text{-H}_2)(\text{PF}(\text{OMe})_2)][\text{BF}_4]_2$  **68** [155]. It is expected that the  $\text{H}_2$  ligand is sensitive to the sterics as well as electronic properties of the *trans*-phosphorous ligands. This trend showed that binding affinity of the phosphine in dihydrogen complexes decreased with an increase in the steric congestion [156]. In another case phosphines in  $\text{trans-}[\text{Ru}(\text{dppe})_2(\eta^2\text{-H}_2)(\text{L})][\text{BF}_4]_2$  (*dppe* =  $\text{Ph}_2\text{PCH}_2\text{CH}_2\text{PPh}_2$ ;  $\text{L} = \text{PMe}_3$  **70**,  $\text{PMe}_2\text{Ph}$  **71**,  $\text{P(O'Pr)}_3$  **72**) were found to be labile with respect to the substitution especially in  $\text{H}_2$  saturated solution and a facile formation of  $\text{trans-}[\text{Ru}(\text{dppe})_2(\text{H})(\eta^2\text{-H}_2)][\text{BF}_4]$  **73** was witnessed under mild condition (Scheme 5).

A very interesting effect of the cone angle reduction of the phosphorous donor  $\text{P}(\text{OMe})_3$  to  $\text{PF}(\text{OMe})_2$  ligands was considered as the major factor for the formation of dihydrogen complexes  $\text{trans-}[\text{Ru}(\text{dppe})_2(\text{H}_2\text{L})][\text{BF}_4]$  ( $\text{L} = \text{PF}(\text{OR})_2$ ) **73**. In the above case, the cone angles of the ligands were obtained based on the computation results using the steric parameters of  $\text{PF}_3$  [157].<sup>1</sup> This fine-tuning in which an interplay of the cone angles (steric crowding around the metal center) and the  $\pi$ -acceptor ability of the *trans* phosphorous ligand were observed. It is to note, in case of the complexes with *trans*- $\text{M}(\text{H})(\eta^2\text{-H}_2)$  moiety, an unusual dynamic process of H-atom site exchange within the dihydrogen and the hydride environment [158] exhibited high barriers whereas *cis* compounds show relatively smaller barriers [5].

Apart from these metals, cobalt also forms a cationic dihydrogen complex  $[(\text{PP}_3)\text{Co}(\eta^2\text{-H}_2)]^+$  ( $\text{PP}_3 = \text{P}(\text{CH}_2\text{CH}_2\text{PPh}_2)_3$  **74**) supported by triphos in which case the formulation was confirmed from the substantial  $^1J_{\text{HD}}$  28 Hz and short  $T_1$  (ms) [159]. Rhodium analogs of the triphos supported  $\text{H}_2$  complexes were reported by Bianchini and co-workers [160]. For a large number of rhodium- $\text{H}_2$  complexes, the absence of H–D coupling in deuterated isotopomers suggested the presence of dihydride in solution in which the isotope perturbation of resonance (IPR) was noted [161]. Addition of  $\text{H}_2$  to a rhodium complex such as  $[\text{Rh}(\text{nod})(\text{PR}_3)_2][\text{BAR}^{\text{F}}_4]$  ( $\text{R} = \text{Cy}$  **75**,  $^i\text{Pr}$  **76**) resulted  $\text{Rh}(\text{III})$  bis-dihydrogen/hydrides  $[\text{Rh}(\text{H})_2(\eta^2\text{-H}_2)_2(\text{PR}_3)_2][\text{BAR}^{\text{F}}_4]$  which loses  $\text{H}_2$  to result in bis-dihydride  $[\text{Rh}(\text{H})_2(\text{L})_2(\text{PR}_3)_2]$  ( $\text{R} = \text{Cy}$  **77**,  $^i\text{Pr}$  **78**,  $\text{L} = \text{CD}_2\text{Cl}_2$  or agostic interaction) [162]. These complexes were characterized by low temperature  $^1\text{H}$  NMR spectroscopy due to the relaxation behavior of the non-classical  $\eta^2\text{-H}_2$  such as noted in the case of thermally unstable and highly fluxional complex  $[(\text{Triphos})\text{Rh}(\eta^2\text{-H}_2)(\text{H})_2]^+$  **79**. This compound contains a fast spinning  $\text{H}_2$  ligand with  $T_{1\text{min}}$  16.5 and 32.6 ms [163]. An interesting fact is that the 2-fold elongation of  $T_{1\text{min}}$  value was observed for the deuterated isotopomers of the parent hydride  $[\text{Ir}(\text{triphos})\text{D}_3]$  **80** to non-classical form  $[(\text{triphos})\text{Ir}(\eta^2\text{-D}_2)(\text{D})]^+$  **81**.

The most unique observation has been that the 5d metal iridium, formed dihydrogen complexes with *elongated* or *compressed* in nature. Coordination of  $\text{H}_2$  to neutral iridium was observed in  $[\text{Ir}(\text{H})_2\text{Cl}(\eta^2\text{-H}_2)(\text{P}^i\text{Pr}_3)_2]$  **82** which manifested the dynamic behavior both in solution and in the solid state [164]. The  $\text{Ir}(\text{III})$  tetrahydrido complex  $[(\text{triphos})\text{Ir}(\eta^2\text{-H}_2)(\text{H})_2][\text{BPh}_4]$  **83** with the labile dihydrogen moiety was characterized in solution by the high pressure  $^1\text{H}$  NMR spectroscopy. This compound was

<sup>1</sup>  $\theta(\text{PF}(\text{OR})_2) = 1/3[\theta(\text{PF}_3)] + 2/3[\theta(\text{P}(\text{OR})_3)]$ .

sufficiently acidic to protonate its counter ion  $\text{BPh}_4^-$  resulting heterolysis of  $\text{H}_2$  [165].

It can be added that there were only limited reports on the Ni and Pd- $\text{H}_2$  complexes such as ligand free  $\text{Pd}(\eta^1\text{-H}_2)$  and  $\text{Pd}(\eta^2\text{-H}_2)$  and end-on and side-on bonded complexes [166]. Caulton and co-workers reported the first dihydrogen complex with  $d^8$  electronic configuration  $[\text{PtH}_3(\text{PBut}_3)_2]^+$  **84** in which oxidative addition of  $\text{H}_2$  afforded a  $d^6$  Pt(IV) species. The protonation of the  $(\text{PCP})\text{PtH}$  ( $\text{PCP} = \eta^3\text{-2,6-(}^t\text{Bu}_2\text{PCH}_2)_2\text{C}_6\text{H}_3$  **85** at  $-78^\circ\text{C}$  afforded the Pt(II) complex  $[(\text{PCP})\text{Pt}(\eta^2\text{-H}_2)]^+$  **86**, where escape of  $\text{H}_2$  was imminent upon warming the solution to room temperature and complex **86** reformed when the  $\text{H}_2$  was reintroduced [167]. Previously, Kubas and co-workers reported a Pt- $\text{H}_2$  complex  $[\text{Pt}(\eta^2\text{-H}_2)(\text{H})(\text{P}^i\text{Pr}_3)_2][\text{BAR}_f]$  ( $\text{BAR}_f = \text{B}(3,5\text{-}(\text{CF}_3)_2\text{C}_6\text{H}_3)_4$ ) **87** with electrophilic counterion [168]. Intensive search revealed that  $\text{Pt}^{\text{II}}$ ,  $\text{Cu}^{\text{II}}$ ,  $\text{Ag}^{\text{II}}$ , and  $\text{Au}^{\text{II}}$  metal ions were not suitable candidate to form bond with  $\text{H}_2$ .

## 5.2. Elongated dihydrogen complexes

Apart from the metal-dihydride and polyhydrides with  $d_{\text{HH}}$  greater or equal to 1.5 Å, complexes with H–H length of 1.0 to 1.6 Å are classified as *elongated* dihydrogen complexes. Structure and bonding features of elongated dihydrogen complexes based on the electronic structure calculations were discussed by Heinekey and co-authors [8]. Complexes in which the H–H bond is elongated are considered as the intermediate species trapped at different stages of the oxidative addition of  $\text{H}_2$  to a metal center. The bonding features of such complexes are unprecedented to the classical bonding principles. Many theoretical [10–14] and experimental [15–20] approaches which advanced the understanding on the unconventional elongated  $\text{H}_2$  complexes and their applications in catalytic processes [21,22]. It is interesting to view the smooth gradation of the H–H distances along the continuum for the oxidative addition of  $\text{H}_2$  to a metal center and investigate at what point the H–H bond is considered to be *broken*. In order to isolate complexes with H–H distances in this continuum a very systematic study is essential by subtly varying the electron donor ability of the coligands such that the  $\text{M}(d\pi) \rightarrow \text{H}_2(\sigma^*)$  electron donation goes up in small increments.

Complex  $[\text{Cp}^*\text{Ru}(\text{dppm})(\text{H}_2)][\text{BF}_4]$  **88** with an elongated  $\text{H}_2$  was structurally characterized by the low-temperature neutron diffraction method which revealed a  $d_{\text{HH}}$  1.10 ± 0.3 Å in good agreement with the H–H distances determined by the spin-lattice relaxation ( $T_1$ ) measurements and the HD spin-spin coupling ( $J_{\text{HD}}$ ) [16]. Later, Heinekey and co-workers have observed that the HD isotopomer of the complex **88** exhibited a small decrease in  $J_{\text{HD}}$  (22.4 to 20.7 Hz) upon increasing the temperature from 200 K to 286 K which resulted a slight increase in H–H distances [20]. This was attributed to the thermal population of the vibrationally excited states to account for the decreased HD coupling at higher temperatures [24]. The DFT formalism using the correlation function Becke3LYP with basis sets LANL2DZ and 6-31G supported the experimental results [24]. A series of dihydrogen complexes  $[\text{Cp}/\text{Cp}^*\text{Ru}(\text{PP})(\eta^2\text{-H}_2)]^+$  ( $\text{PP} = \text{chelating diphosphine}$ ) with HD coupling constants  $J_{\text{HD}}$

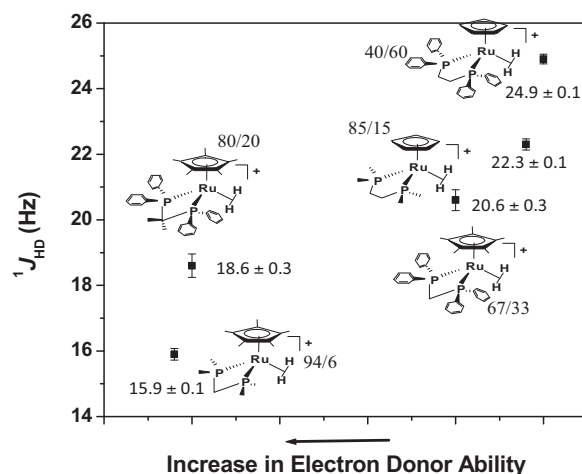


Fig. 5. A series of dihydrogen complexes of the type  $[\text{Cp}/\text{Cp}^*\text{Ru}(\text{PP})(\eta^2\text{-H}_2)]^+$  with their  $(\eta^2\text{-H}_2)/(\text{H})_2$  ratio where a decrease in  $J_{\text{HD}}$  (Hz) [19] upon increasing electron donor ability of the bisphosphine represented by the arbitrary X-axis.

(20.6 ± 0.3 to 15.9 ± 0.1 Hz, Fig. 5) and  $d_{\text{HH}}$  1.0 to 1.15 Å including the errors in  $J_{\text{HD}}$  measurements [110] showed temperature and isotope dependence coupling constants [19]. The subtle effect of the electron donor ability of the bisphosphines was reflected in decrease in  $J_{\text{HD}}$  which significantly affect the vibrational potential of the  $\eta^2\text{-H}_2$  [19].

For another set of complexes,  $\text{trans-}[\text{M}(\eta^2\text{-H}_2)(\text{Cl})(\text{PP})_2]^+$  where ( $\text{M} = \text{Ru}$  and  $\text{Os}$ , and  $\text{PP} = \text{R}_2\text{PCH}_2\text{CH}_2\text{PR}_2$ ,  $\text{R} = \text{Ph}$ ,  $\text{Et}$ , and  $\text{Cy}$ ), elongation of H–H bond with increase of electron density on the metal center was observed [110]. The H–H distance increased from 0.99 to 1.15 Å (Ph to Cy) for ruthenium and 1.19 to 1.24 Å (Ph to Cy) for osmium series which suggested the occupation of electron density on the  $\sigma^*$  orbital of the  $\eta^2\text{-H}_2$  resulting an elongation of H–H bond (Fig. 6). The fine-tuning of the electron density by subtle balance of electronics of phosphine resulted in small changes in  $d_{\text{HH}}$  (Fig. 6).

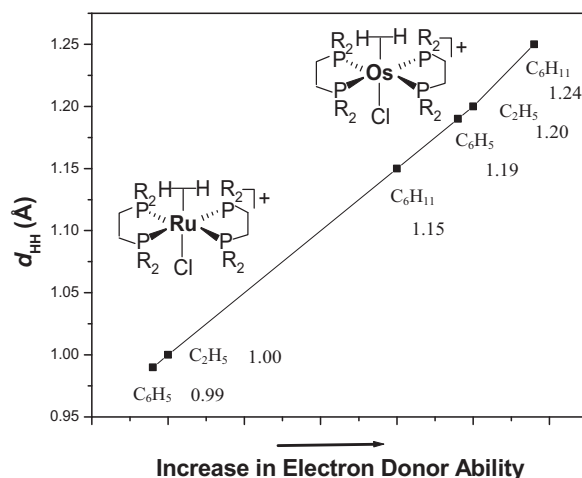
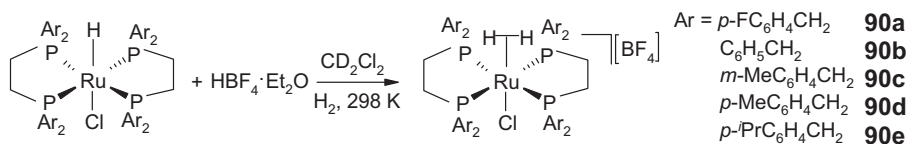


Fig. 6. Plot of increments in H–H distances ( $d_{\text{HH}}$ , Å obtained from  $J_{\text{HD}}$  excluding the errors in measurements) with increase in electron donor ability of the bisphosphine (arbitrary X axis; phenyl to cyclohexyl) for 3d and 5d transition metal dihydrogen complexes [110].





Scheme 6. Dihydrogen complexes  $trans\text{-}[\text{Ru}(\eta^2\text{-H}_2)\text{Cl}](\text{PP})_2[\text{BF}_4]$  obtained from corresponding hydrides [23].

A structural characterization of  $trans\text{-}[\text{Os}(\text{H}_2)(\text{Cl})(\text{dppe})_2]^+$  **89** using the neutron diffraction method gives a  $d_{\text{HH}} = 1.22 \pm 0.3 \text{ \AA}$  which was consistent with the  $^1J_{\text{HD}}$  ca. 14 Hz measured by  $^1\text{H}$  NMR spectroscopy. In this case, the HD coupling constants ( $^1J_{\text{HD}}$  Hz) showed modest temperature dependence exhibiting a slight increase in  $^1J_{\text{HD}}$  with increase in temperature, i.e. average H–H bond distance decreases at higher temperatures [127]. Generally, *elongated*  $\text{H}_2$  complexes of Ru, Os, and Re supported with phosphines showed HD spin-spin coupling constant 5–25 Hz. Calculated H–H bond energy (100 to 190  $\text{kJ mol}^{-1}$ ) of the elongated  $\text{H}_2$  complexes using the Becke3LYP method and LANL2DZ basis set has been larger than that of the classical  $\eta^2\text{-H}_2$  complexes (60–85  $\text{kJ mol}^{-1}$ ) [8].

More recently, we reported synthesis and characterization of a series of  $\text{H}_2$  complexes bearing bis(1,2-diarylphosphino)ethane in which the aryl group was a benzyl moiety with a substituent (*p*-fluoro, H, *m*-methyl, *p*-methyl, *p*-isopropyl) (Scheme 6) [23]. The donor ability of the chelating phosphine was increased in small increments along the series in  $trans\text{-}[\text{Ru}(\eta^2\text{-H}_2)(\text{Cl})(\text{PP})_2][\text{BF}_4]$  (**90a–e**), resulting in a moderate elongation of H–H bonds from 0.97 to 1.03  $\text{\AA}$  [23]. The  $d_{\text{HH}}$  was calculated using the Morris empirical relation constructed by using the H–H distances from various structural studies of the dihydrogen complexes using X-ray, neutron diffraction, and solid state NMR [110]. The systematic small increments in H–H distances appeared as the snapshots of the *breaking* of the H–H bond in the process of OA of  $\text{H}_2$  [23] (Fig. 7).

Small increments in H–H distances with the increase in electron donor ability of the chelating phosphine was correlated with the appropriate Hammett substituent

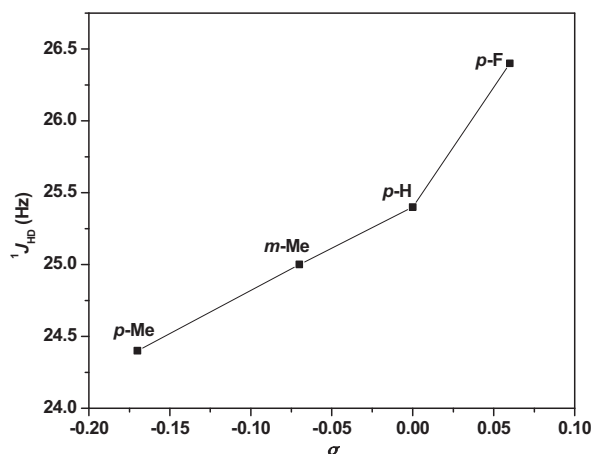


Fig. 7. Plot of  $^1J_{\text{HD}}$  of HD isotopomer versus Hammett constants ( $\sigma$ ) of the benzyl ligand (figure was reproduced from Ref. [23], Copyright (2008) American Chemical Society).

constants ( $\sigma$ ), *p*-F (0.06), H(0), *m*-CH<sub>3</sub> (–0.07), *p*-CH<sub>3</sub> (–0.17), *p*-<sup>i</sup>Pr (not available) [23] (and references there in) i.e. increase in H–H distance along the order  $\text{Ar} = p\text{-FC}_6\text{H}_4 < \text{C}_6\text{H}_5 < m\text{-CH}_3\text{C}_6\text{H}_4 < p\text{-CH}_3\text{C}_6\text{H}_4 < p\text{-}^i\text{PrC}_6\text{H}_4$  which was represented by a  $^1J_{\text{HD}}$  versus  $\sigma$  (benzyl group) plot in Fig. 5. One of the  $\text{H}_2$  complexes  $trans\text{-}[\text{Ru}(\eta^2\text{-H}_2)(\text{Cl})((\text{C}_6\text{H}_5\text{CH}_2)_2\text{PCH}_2\text{CH}_2\text{P}(\text{CH}_2\text{C}_6\text{H}_5)_2)_2][\text{BF}_4]$  **90b** was structurally characterized by X-ray diffraction. The ORTEP diagram of the cation is shown in Fig. 8.

A number of representative *elongated* dihydrogen complexes and their H–H distances are listed in Table 1.

A osmium complex  $[\text{OsClH}_3(\text{PPh}_3)_3]$  **3** with highly stretched H–H moiety, holds a suitable sterics around the metal center provided by the three triphenyl phosphine ligands. Neutron diffraction structure of **3** revealed a dihydrogen-hydride character and an *elongated*  $\text{H}_2$  with a H–H distance of 1.48(2)  $\text{\AA}$  as shown in Fig. 9. A short spin-lattice relaxation time ( $T_1$  26 ms) at  $-40^\circ\text{C}$  (300 MHz  $^1\text{H}$  NMR) also supported a dihydrogen-hydride character [15]. This and other similar studies on H–H elongation influenced by the electronic and sterics of phosphine perhaps directs a correlation of H...H coupling constants ( $^1J_{\text{HH}}$ ) and distances ( $d_{\text{HH}}$ ) measured from the neutron structure and compare them with the  $^1\text{H}$  NMR results. Jia and coworkers summarized neutron diffraction determined H–H distances of metal- $\text{H}_2$  complexes which determines a reaction coordinate for the oxidative addition  $\text{H}_2$  on a metal center [15].

In another study, a positively charged highly acidic iridium complex  $[\text{Cp}^*\text{Ir}(\text{dmpm})\text{H}_2]^+$  **4** supported by electron donating  $\text{Cp}^*$  and bis-phosphine resulted a mixture of elongated  $\text{H}_2$  complex and *cis*-dihydride.

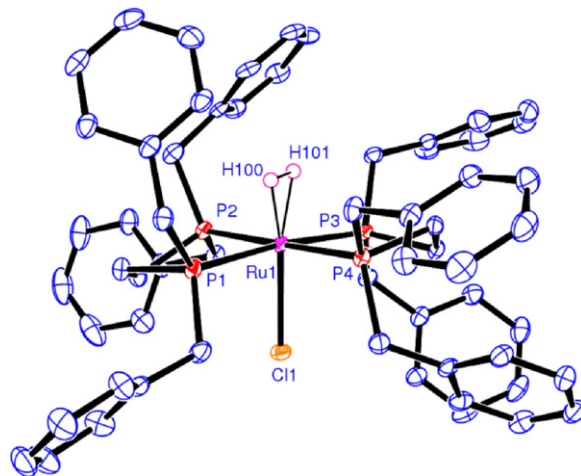


Fig. 8. ORTEP view of  $trans\text{-}[\text{Ru}(\eta^2\text{-H}_2)(\text{Cl})((\text{C}_6\text{H}_5\text{CH}_2)_2\text{PCH}_2\text{CH}_2\text{P}(\text{CH}_2\text{C}_6\text{H}_5)_2)_2][\text{BF}_4]$  **90b** at the 50% probability level (figure was reproduced from Ref. [23], Copyright (2008) American Chemical Society).

**Table 1**  
Representative *elongated* dihydrogen complexes.

Entry	Compounds	$^1J_{\text{HD}}$ (Hz)	$d_{\text{HH}}$ (Å)	Ref.
1	$[\text{OsClH}_3(\text{PPh}_3)_3]$ <b>3</b>		1.48(2) (N)	[15]
2	$[\text{Cp}^*\text{Ir}(\text{dppm})\text{H}_2]^{+2}$ <b>4</b>	7.0–9.0	1.38–1.31	[18]
3	$[\text{Re}(\text{H}_2)(\text{NO})\text{Br}_2(\text{P}^i\text{Pr}_3)_2]$ <b>91</b>	12.8	1.23	[25]
4	$[\text{Os}(\text{dppe})_2\text{Cl}(\text{H}_2)]^+$ <b>89</b>	13.6–14.2	1.21–1.20	[110]
5	$[\text{Cp}'_2\text{Nb}(\text{PMe}_2\text{Ph})(\text{H}_2)]^+$ <b>92</b>	15	1.22(3) (N)	[26]
6	$[\text{OsCl}(\text{NH}=\text{C}(\text{Ph})\text{C}_6\text{H}_4)(\text{P}^i\text{Pr}_3)_2(\text{H}_2)]$ <b>93</b>	6.8	1.17	[27]
			1.39	[27]

Values from neutron diffraction measurements are indicated by (N). Errors in H–H distances are noted wherever reported.

Measured HD coupling constant 8.1 Hz of the deuterated isotopomer of **4** at 303 K corresponds to a  $d_{\text{HH}}$  1.34 Å [18,110].

In contrast, a classical and nonclassical nitrosyl hydride complex of rhenium exists in different oxidation states. A nitrosyl complex  $[\text{Re}(\text{Br})_2(\text{NO})(\eta^2\text{-H}_2)(\text{P}^i\text{Pr}_3)_2]$  **91** with an elongated H...H moiety exhibited a  $^1J_{\text{HD}}$  12.8 Hz of the HMD isotopomer which corresponds to a 1.27 Å H–H distance [130]. Similarly, a Nb–H<sub>2</sub> complex  $[\text{Cp}'_2\text{Nb}(\text{PMe}_2\text{Ph})(\text{H}_2)]^+$  **92** contains an intact H<sub>2</sub> ligand with a H–H distance 1.17 Å [131]. Slowly rotating HD bound to the Nb center in which the two interconverting rotamers were identified by the <sup>1</sup>H NMR study. An osmium complex  $[\text{OsCl}(\text{NH}=\text{C}(\text{Ph})\text{C}_6\text{H}_4)(\text{P}^i\text{Pr}_3)_2(\eta^2\text{-H}_2)]$  **93** with an *elongated* H<sub>2</sub> ( $d_{\text{HH}}$  1.39 Å) also exhibited a restricted rotational motion in solution. Such rotational barrier was dependent on the electron donor ability of the *trans* ligand to H<sub>2</sub> (Cl, Br, H etc.) and H–H distances were found to be temperature dependent.

Heinekey and co-workers elucidated the nature of the H–H bond in *elongated* dihydrogen complexes and the effect of temperature variation on the H–H distances. The compounds which were studied for the temperature dependence of the  $^1J_{\text{HD}}$  and  $d_{\text{HH}}$ , for example  $[\text{Cp}^*\text{Ru}(\text{dppm})(\text{H}_2)]^+$  **89** that exhibited a small decrease in  $^1J_{\text{HD}}$  upon increasing the temperature from 200 K to room temperature. This reflected in the increase of H–H (H–D) distances [11]. In verification of the temperature dependence of the coupling and probing the isotope effects on the bond distances, <sup>3</sup>H NMR spectroscopy has

been an advantageous tool for determining H–T coupling. It was observed that the bond distances calculated from <sup>1</sup>H NMR data was in good agreement with that obtained from neutron diffraction studies for  $[\text{Cp}^*\text{Ru}(\text{dppm})(\text{H}_2)]^+$  **89**. Temperature dependent coupling constants also suggested rapid equilibrium between the predominant dihydrogen and a minor *cis*-dihydride tautomer.

Next to the experimental results, Lluch and co-workers predicted the temperature dependence of the coupling constants for the complex  $[\text{Cp}^*\text{Ru}(\text{dppm})(\text{H}_2)]^+$  **89** based on the realistic theoretical model of  $[\text{Cp}^*\text{Ru}(\text{H}_2\text{PCH}_2\text{CH}_2\text{PH}_2)(\text{H}_2)]^+$  **94** derived by the electronic structure calculations using DFT at the B3LYP level [24]. Theoretical results predicted the increase in H–H distances at higher temperatures on the grounds of varying population of the vibrational excited states of the Ru–H<sub>2</sub> unit. Interestingly, complex *trans*- $[\text{Os}(\text{H}-\text{H})(\text{Cl})(\text{dppe})_2]^+$  **90** exhibited a temperature dependent coupling constants ( $J_{\text{HD}}$ ) such as 13.6 Hz at 253 K; 14.2 Hz at 308 K. This complex exhibited an inverse variation of the  $^1J_{\text{HD}}$  with the temperature. The Boltzman averaged discrete variable representations (DVR) was applied for the calculations within a considerable number of dimensions [29]. This revealed that upon an increase in temperature certain excited vibrational states were populated that would lead to a decrease of the mean thermal H–H distances. This was consistent with the increase in  $^1J_{\text{HD}}$  at higher temperatures [14]. An energy profile (Fig. 10) for the lengthening of the H–H bond while relaxing the rest of the structure for a theoretical model of  $[\text{CpRu}(\text{H}_2\text{PCH}_2\text{CH}_2\text{PH}_2)(\text{H}_2)]^+$  **95** was obtained from

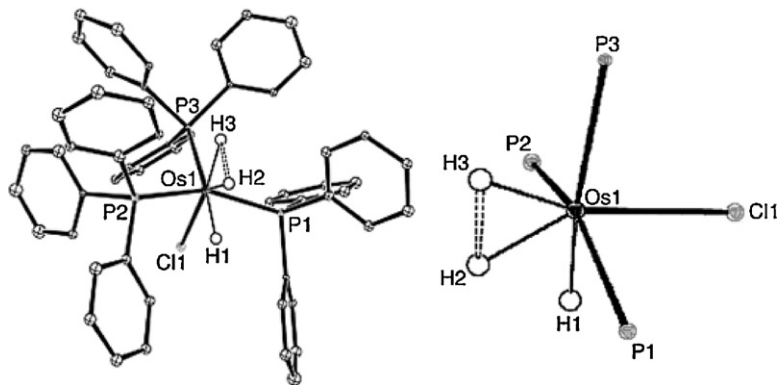


**Fig. 9.** Molecular structure of  $[\text{OsClH}_3(\text{PPh}_3)_3]$  (**3**, left) and its core (right). The H<sub>2</sub>–H<sub>3</sub> distance is 1.48(2) Å and the H<sub>1</sub>...H<sub>2</sub> distance is 1.67(2) Å, as determined from this neutron study. Other notable bond distances include: Os–H<sub>2</sub> = 1.59(2) and Os–H<sub>3</sub> 1.61(1) Å (figure was reproduced from Ref. [15], Copyright (2005) Wiley–VCH Verlag GmbH & Co. KGaA).

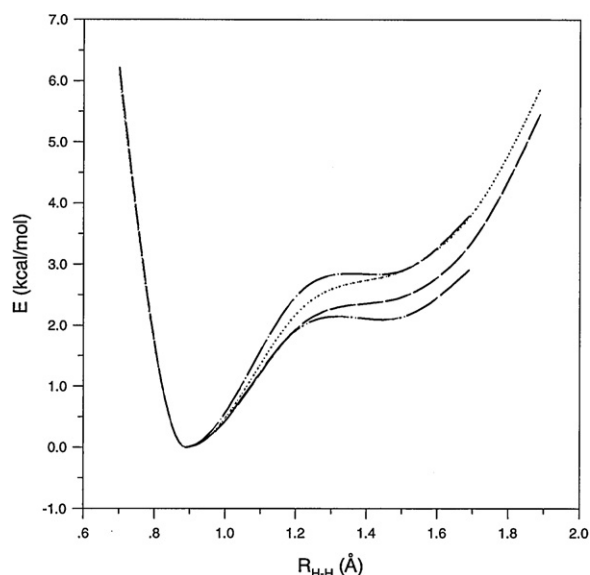


Fig. 10. Energy profiles for the lengthening of the H–H bond while relaxing the rest of the structure in the complex  $[\text{RuH}_2(\text{C}_5\text{H}_5)(\text{H}_2\text{PCH}_2\text{PH}_2)]^+$ , at different calculational levels: (from top to bottom) CCSD//B3LYP (dash–dot), B3LYP\*/B3LYP (dot–dot), B3LYP//B3LYP (dash–dash), and CCSD(T)//B3LYP (dash–dot–dot). B3LYP\* refers to B3LYP calculations performed with polarization functions on all heavy atoms (figure was reproduced from Ref. [24], Copyright (1997) American Chemical Society).

electronic structure calculations using DFT at B3LYP level and also at CCSD and CCSD(T) levels [24].

The dynamics of the Ru–H<sub>2</sub> unit being the major concern in evaluation of the potential energy surface (PES) corresponding to the motion of the Ru–H<sub>2</sub> unit. In this context, Lluch and co-workers constructed the 2D PES (Fig. 11) and solved by using the DVR techniques by constructing the matrix representation of the Hamiltonian corresponding to the nuclear motion [24]. The expectation values obtained for both the parameters ( $R_{\text{H-H}} = 1.02 \text{ \AA}$ ,  $R_{\text{Ru-H}_2} = 1.61 \text{ \AA}$ ) were in good agreement with neutron diffraction result ( $R_{\text{H-H}} = 1.10 \text{ \AA}$ ,  $R_{\text{Ru-H}_2} = 1.58 \text{ \AA}$ ) [13] than the structural parameters corresponding to the PES minimum ( $R_{\text{H-H}} = 0.89 \text{ \AA}$ ,  $R_{\text{Ru-H}_2} = 1.66 \text{ \AA}$ ) [24].

We studied the temperature dependence of the HD coupling constant for the complex  $[\text{Ru}(\eta^2\text{-H}_2)((\text{C}_6\text{H}_5\text{CH}_2)_2\text{PCH}_2\text{CH}_2\text{P}(\text{CH}_2\text{C}_6\text{H}_5)_2)]\text{[OTf]}_2$  **17** exhibiting a modest variation from 22.0 Hz at 293 K to 24.0 Hz at 233 K [31]. Similar was observed for most of the *elongated* dihydrogen complexes [8]. Pronounced temperature dependence of  $^1J_{\text{HD}}$ 's was opposite to that observed for  $[\text{Cp}^*\text{Ru}(\text{dppm})\text{H}_2]^+$  **89**. It was found that coupling increases at higher temperature suggesting a decrease in H–H distances. The large temperature dependent isotope shifts were also noted. This indicates non-statistical occupation of deuterium versus H atoms in more than one distinct structure [19]. The quantum mechanical calculations (resolution of the electronic Schrödinger equation and geometry optimization) suggested that flat minimum potential energy surface (PES) with the H–H distance, influenced by the librational motion. A more prominent temperature effect

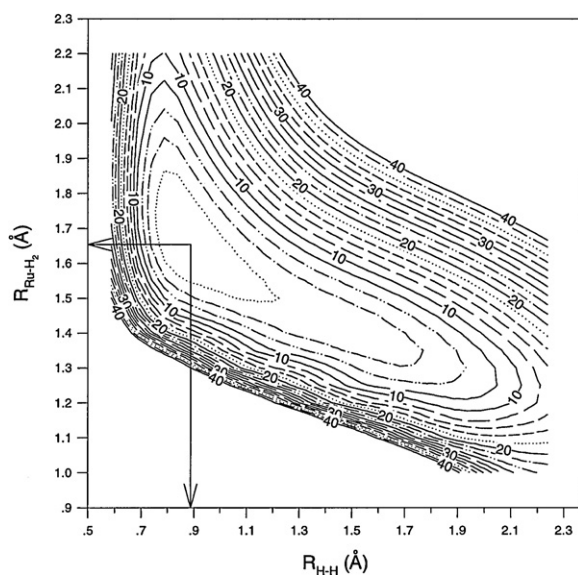


Fig. 11. Contour plot of the 2D PES for the complex  $[\text{RuH}_2(\text{C}_5\text{H}_5)(\text{H}_2\text{PCH}_2\text{CH}_2\text{PH}_2)]^+$ . Energy contours appear every  $2 \text{ kcal mol}^{-1}$ . The arrows indicate the position of the minimum in potential energy ( $R_{\text{H-H}} = 0.89 \text{ \AA}$ ,  $R_{\text{Ru-H}_2} = 1.66 \text{ \AA}$ ) (figure was reproduced from Ref. [24], Copyright (1997) American Chemical Society).

was noted for the iridium complex  $[\text{Cp}^*\text{Ir}(\text{dmpm})\text{H}]^+$  **4**. Detailed analysis of the potential energy surface (PES) of the metal bound  $\eta^2\text{-H}_2$  is necessary in order to predict the temperature dependence of the  $^1J_{\text{HD}}$  and H–H distances so also the experimental observation to distinguish the elongated dihydrogen complexes from the compressed dihydrides.

A density functional electronic structure calculations using B3LYP method and LANL2DZ, 31G(d), 31G(p), 6-31G basis sets for the different atoms in combination with quantum nuclear dynamical calculations by choosing the generic DVR for the model complexes  $[\text{Cp}^*\text{Ru}(\text{H}_2\text{PCH}_2\text{CH}_2\text{PH}_2)(\text{H}_2)]^+$  **93** and  $[\text{CpRe}(\text{CO})_2\text{H}_2]$  **94** provided information on the metal–H<sub>2</sub> unit, its nuclear motion, and temperature dependence of the H–D spin-spin coupling constant ( $^1J_{\text{HD}}$ ) [11]. Calculations on the model complex  $[\text{Cp}^*\text{Ru}(\text{H}_2\text{PCH}_2\text{CH}_2\text{PH}_2)(\text{H}_2)]^+$  **93** revealed (Contour plots, Fig. 12) an increase in  $R_{\text{H-H}}$  with temperature, in contrast to that observed in the case of complex  $[\text{CpRe}(\text{CO})_2\text{H}_2]$  **96** [11].

It was found that the complexes  $[\text{Cp}^*\text{Ir}(\text{dmpm})\text{H}_2]^+$  **4**,  $[\text{Cp}^*\text{Ru}(\text{dppm})(\text{H}_2)]^+$  **94**, and  $[\text{CpRe}(\text{CO})_2\text{H}_2]$  **96** share striking similarities in terms of  $^1\text{H}$  NMR chemical shifts and  $^1J_{\text{HD}}$  values. This fact was explained in terms of location of the potential energy minimum and the deformation of the H–H distance. Two different families of elongated dihydrogen complexes with strong dihydrogen character (large  $^1J_{\text{HD}}$  values) and potential energy (PE) minimum, exhibited increase in dihydrogen character with increase in temperature. The complexes with PE minimum and strong dihydride character (small  $^1J_{\text{HD}}$ ) in which a decrease in  $d_{\text{HH}}$  was observed with increase in temperature. In case of the deuterated HD isotopomers of complexes  $[\text{Cp}^*\text{Re}(\text{CO})_2\text{H}_2]$  **96** and  $[\text{Cp}^*\text{Ir}(\text{dmpm})\text{H}_2]^+$  **4**, a decrease in  $d_{\text{HH}}$  was eminent

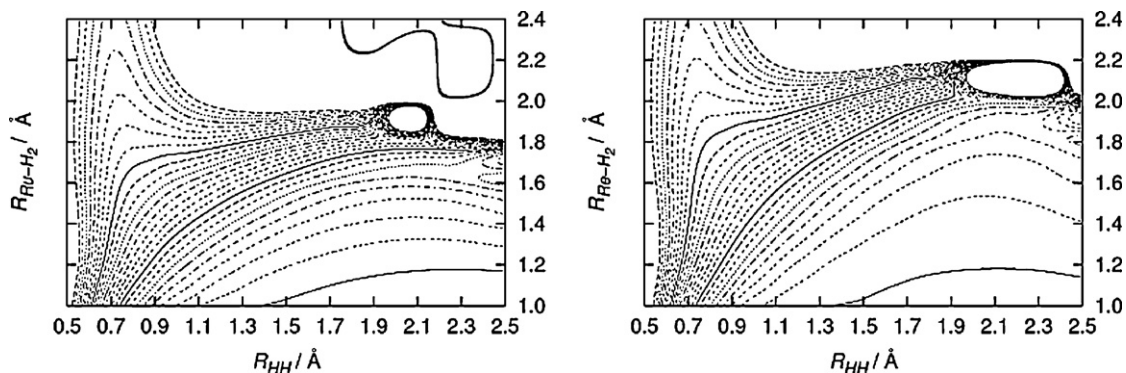


Fig. 12. Contour plots of  $^1J_{\text{HD}}$  for complexes **93** and **96** starting at 2 Hz and increase in 2 Hz intervals (figure was reproduced from Ref. [11], Copyright (2005) Wiley-VCH Verlag GmbH & Co. KGaA).

whereas for the compressed dihydrides, an increase in  $d_{\text{HH}}$  was evidenced [18].

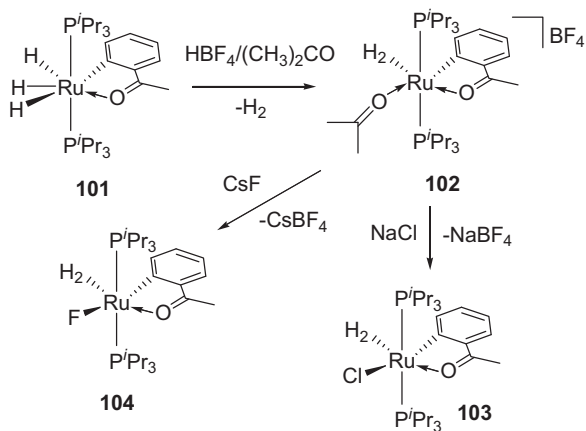
Elongated dihydrogen and compressed dihydride complexes were differentiated based on the theoretical findings of the temperature dependence of  $^1J_{\text{HD}}$ ,  $d_{\text{HH}}$ , and isotope dependence of the H–H distances [11]. Similarly the hypothesis of decreased coupling at higher temperature due to the thermal population of vibrationally excited states was experimentally verified for a series of complexes  $[\text{Cp}/\text{Cp}^*\text{Ru}(\text{PP})(\text{H}_2)]^+$  ( $\text{Cp}^*$  and  $\text{PP} = \text{dppm}$  **94**,  $\text{Cp}^*$  and  $\text{PP} = \text{dmppm}$  **97**,  $\text{Cp}$  and  $\text{PP} = \text{dppe}$  **98**,  $\text{Cp}$  and  $\text{PP} = \text{dmpe}$  **99**,  $\text{Cp}^*$  and  $\text{PP} = \text{dppip}$  **100**) existed as slowly equilibrating mixtures of *trans*-dihydride and dihydrogen tautomers. In the above case, a greater elongation of the H–H distance would result in a softer potential for the  $\text{H}_2$  unit and give

rise to greater effect of temperature on bond lengths. In this series, complexes  $[\text{Cp}^*\text{Ru}(\text{dmpm})\text{H}_2]^+$  **97** and  $[\text{Cp}^*\text{Ru}(\text{dppip})\text{H}_2]^+$  **100** [19] contain high electron density on the metal which reflected in smaller  $^1J_{\text{HD}}$ 's  $18.6 \pm 0.3$  and  $15.9 \pm 0.1$  Hz indicating considerable elongation of H–H distances and temperature invariant H–D coupling. In this case, the thermal population of the vibrationally excited states was not accompanied by the elongation of the H–H bond. The examination of the H–D coupling as a function of temperature for the complex  $[\text{CpRu}(\text{dmpe})\text{H}_2]^+$  **97** [19] revealed a modest variation of 23 Hz at 200 K to 22.3 Hz at 300 K. It also pointed out that temperature dependence of the H–P coupling in  $[\text{CpRu}(\text{dmpe})\text{H}_2]^+$  **97** was due to the thermal population of a vibrational excited state, leading to more efficient transmission of  $^1\text{H}-^{31}\text{P}$  coupling. However, temperature dependence can be a sensitive indicator of H–H bond stretching due to the thermal excitation of low energy vibrational modes [24].

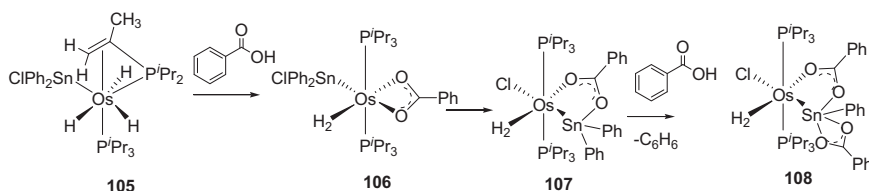
Along with the structural studies of  $\text{H}_2$  complexes, both theoretical and experimental findings on their reactivity were essential. In this direction, osmium complexes with considerably elongated  $\text{H}_2$  ligand were utilized as templates for C–C and C–heteroatom coupling reactions (Scheme 7) [32].

The H–H distances 1.36 and 1.35 Å of complexes **103** and **104** respectively calculated from HD coupling studies were shorter than the H–H distances (1.49(6) Å) of **102** determined by X-ray. Further studies on the similar osmium systems revealed the formation of dihydrogen complexes **106**, **107**, and **108** with four and five coordinated tin centers (Scheme 8) [33].

A  $T_1$  (min) of  $74 \pm 1$  ms of **106** at 243 K corresponds to a 1.50 Å H–H distance assuming slow spinning rate which was



Scheme 7. Preparation of the reactive dihydrogen complexes [32].



Scheme 8. Preparation of the Sn coordinated dihydrogen complexes [33].



consistent with the *elongated* H<sub>2</sub>. X-ray structural study revealed the H–H separation of 1.39 and 1.52 Å for complexes **107** and **108** respectively. Study by Esteruelas and co-workers revealed a different kind of reactivity of elongated H<sub>2</sub> complex by reacting [Os{C<sub>6</sub>H<sub>4</sub>C(O)CH<sub>3</sub>}(η<sup>2</sup>-H<sub>2</sub>){N(OH)=CMe<sub>2</sub>}(P<sup>t</sup>Pr<sub>3</sub>)<sub>2</sub>]<sup>+</sup> **109** (d<sub>H–H</sub> = 1.3 Å) with terminal alkynes resulting dihydride-carbenes [34] whereas water complexes [Os{C<sub>6</sub>H<sub>4</sub>C(O)CH<sub>3</sub>}(η<sup>2</sup>-H<sub>2</sub>)(H<sub>2</sub>O)(P<sup>t</sup>-Pr<sub>3</sub>)<sub>2</sub>][BF<sub>4</sub>] (X = F **110**, H **111**; d<sub>H–H</sub> = 1.3 Å) yielded hydride-vinylidene-π-alkyne derivative and/or hydride-osmacyclopropene species in a competitive manner [35]. Furthermore, hydride-dihydrogen complex OsH(η<sup>2</sup>-H<sub>2</sub>)(η<sup>2</sup>-CH<sub>2</sub>=CH-o-C<sub>5</sub>H<sub>4</sub>N)(P<sup>t</sup>Pr<sub>3</sub>)<sub>2</sub>][BF<sub>4</sub>] **112** was active in CH activation of various carbonyl substrates such as aromatic ketones and olefinic C(sp<sup>2</sup>)-H bond of α,β-unsaturated ketones [36].

### 5.3. Cis-M(dihydrogen)(hydride) complexes

The study related to transition metal polyhydride complexes is a topic of interest [5,7,37–40] because of their structural diversity and dynamic behavior involving multiple hydride ligands. These were extensively studied in homogeneous catalysis, including hydrogenation of the unsaturated compounds [41]. They adopt either classical structure with terminal hydrides or exist in non-classical forms with one or more η<sup>2</sup>-H<sub>2</sub> ligand. The major interests have been focused on the dynamics of the complexes which are prototypical of the larger class of polyhydrides. Most of these compounds exhibited rapid exchange of H-atoms between the dihydrogen and hydride nuclei, as revealed by variable temperature NMR spectroscopic studies. Crabtree reported the dynamic behavior of the iridium complex [Ir(H)(η<sup>2</sup>-H<sub>2</sub>)(bq)(PPh<sub>3</sub>)<sub>2</sub>]<sup>+</sup> **8** (bq = benzoquinolate) which undergoes hydrogen atom exchange between the dihydrogen and hydride ligands with an exchange barrier ΔG<sup>‡</sup><sub>240</sub> = 10 kcal mol<sup>-1</sup> [42]. Bampos et al. reported an iron complex [Fe(H)(H<sub>2</sub>)[P(CH<sub>2</sub>CH<sub>2</sub>CH<sub>2</sub>-PMe<sub>2</sub>)<sub>3</sub>]<sup>+</sup> **9** with exchange barrier of ΔG<sup>‡</sup><sub>240</sub> = 9.1 kcal mol<sup>-1</sup> for the permutation of the hydrogen environments (Fig. 2) [43]. Similarly, Oldham et al. reported an iridium complex [Ir(H)(Tp<sup>R2</sup>)(H<sub>2</sub>)(PMe<sub>3</sub>)]<sup>+</sup> (R = H) (Tp = hydrotris(1-pyrozyl)borate) **10** (Fig. 2) exhibiting a rapid exchange of H atoms within dihydrogen and hydride environments [44]. Large temperature dependent isotope shifts were noted for the hydride resonances of the deuterated isotopomers. The activation energy for the H-atom exchange was calculated to be ΔG<sup>‡</sup> ≤ 5 kcal mol<sup>-1</sup> at 127 K from the limiting spectroscopic parameters of a deuterated sample [44]. For the deuterated isotopomers **10-d**<sub>1</sub> and **10-d**<sub>2</sub>, the calculated <sup>1</sup>J<sub>H–D</sub> 31.5 Hz [46] corresponds to a H–H distance of 0.90 Å. Assuming the deuterium atoms distributed statistically in a dihydrogen/hydride structure, further examination revealed that sufficiently rapid exchange causes irresolvable limiting <sup>1</sup>H NMR chemical shifts for the H and H<sub>2</sub> nuclei even at very low temperature (158 K). The estimated barrier of the H-atom site exchange was less or equal to 4.5 kcal mol<sup>-1</sup> for the complex **11** as obtained from isotope perturbation studies [46]. Heinekey and coworkers had reported the H-atom exchange behavior of the dihydrogen-hydride complexes [Ru(H)(H<sub>2</sub>)(bipy)(PCy<sub>3</sub>)<sub>2</sub>][BAR<sub>4</sub>] **12** (bipy = 2,2'-bipyridine)

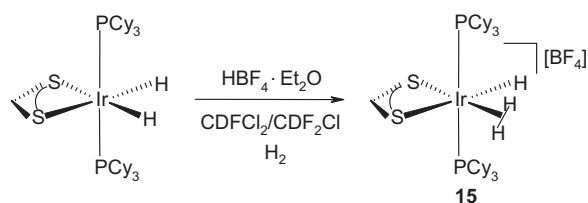
and [Ru(H)(H<sub>2</sub>)(phen)(PCy<sub>3</sub>)<sub>2</sub>][BAR<sub>4</sub>] **13** (1,10-phenanthroline) (Ar = 3,5-(CF<sub>3</sub>)<sub>2</sub>C<sub>6</sub>H<sub>3</sub>) (Fig. 2). The H–H (d<sub>H–H</sub>) distance of these complexes were calculated as 1.1–1.2 Å [110] and the measured <sup>1</sup>J<sub>HD</sub>'s of 19 and 17 Hz gives an exchange barrier of ΔG<sup>‡</sup><sub>128</sub> ≤ 5.0 kcal mol<sup>-1</sup> [44,45]. In case of the CO complex *cis*-[Ru(H)(H<sub>2</sub>)(PCy<sub>3</sub>)<sub>2</sub>(CO)<sub>2</sub>]<sup>+</sup> **14**, exchange barrier ΔG<sup>‡</sup><sub>128</sub> = 5.5 kcal mol<sup>-1</sup> at 130 K was calculated from <sup>13</sup>C NMR spectrum [45]. The effect of electrophilicity of CO upon the H–H distances is an extremely important factor governing the activation energy of the site exchange process between dihydrogen and hydride ligands. The shortening of H–H distance (0.90 Å) by the influence of CO resulting increase in acidity of the metal center was reflected in case of *cis*-[Ru(H)(H<sub>2</sub>)(PCy<sub>3</sub>)<sub>2</sub>(CO)<sub>2</sub>]<sup>+</sup> **14**.

In a *cis*-dihydrogen-hydride complex, H-atom exchange between the dihydrogen and hydride environments requires significant rearrangement of the ancillary ligands which is expected to contribute substantially to the activation energy of the process [110]. A *cis*-[Ir(H)<sub>2</sub>(η<sup>2</sup>-S<sub>2</sub>CH)(PCy<sub>3</sub>)<sub>2</sub>] dihydride with a dithioformate moiety was synthesized by the insertion of the CS<sub>2</sub> into the Ir–H of [Ir(H)<sub>5</sub>(PCy<sub>3</sub>)<sub>2</sub>] [47]. Upon protonation with HBF<sub>4</sub>·Et<sub>2</sub>O at room temperature, H-atom undergoes site exchange between dihydrogen and hydride in *cis*-[Ir(H)(η<sup>2</sup>-H<sub>2</sub>)(η<sup>2</sup>-S<sub>2</sub>CH)(PCy<sub>3</sub>)<sub>2</sub>][BF<sub>4</sub>] **15** with minimum movement of the ancillary ligands (Scheme 9).

Partial deuteration resulted in H<sub>2</sub>D and HD<sub>2</sub> isotopomer of *cis*-[Ir(H)(η<sup>2</sup>-H<sub>2</sub>)(η<sup>2</sup>-S<sub>2</sub>CH)(PCy<sub>3</sub>)<sub>2</sub>][BF<sub>4</sub>] with <sup>1</sup>J<sub>HD</sub>'s of 6.5 and 7.7 Hz from which corresponds to the H–H distance 1.05 Å by using d<sub>H–H</sub>-<sup>1</sup>J<sub>HD</sub> relation [110]. The conclusive evidence supporting the fluxionality of trihydride or a dihydrogen/hydride was obtained from the variable temperature spin-lattice relaxation time (T<sub>1</sub>) measurements. The short T<sub>1</sub> (ms) values of **15**, supported an intact H<sub>2</sub> bound to the metal. The plots of temperature dependent T<sub>1</sub> (ms) for the dihydride and dihydrogen-hydride complexes are given in Fig. 13.

Upon purging with D<sub>2</sub> gas for prolonged period of time, deuterated isotopomers H<sub>3</sub>, H<sub>2</sub>D and HD<sub>2</sub> of **15** resulted. The resonances due to the H<sub>2</sub>D and HD<sub>2</sub> species showed downfield shift with respect to that of the H<sub>3</sub> by Δδ = 97 and 49 ppb (273 K) and 153 and 71 ppb (193 K), respectively suggesting the isotopic perturbation due to the nonstatistical distribution of deuterium. A <sup>1</sup>H NMR plot of the hydride region of deuterated **15** at 263 K (500 MHz) is shown in Fig. 14.

The isotope perturbation may cause the isotope shifts within dihydrogen/hydride ground-state structure where deuterium incorporation occurred in a particular site. The temperature-dependent downfield chemical shift was



Scheme 9. Dithioformate dihydrogen-hydride complex formation from corresponding *cis*-dihydride [47].



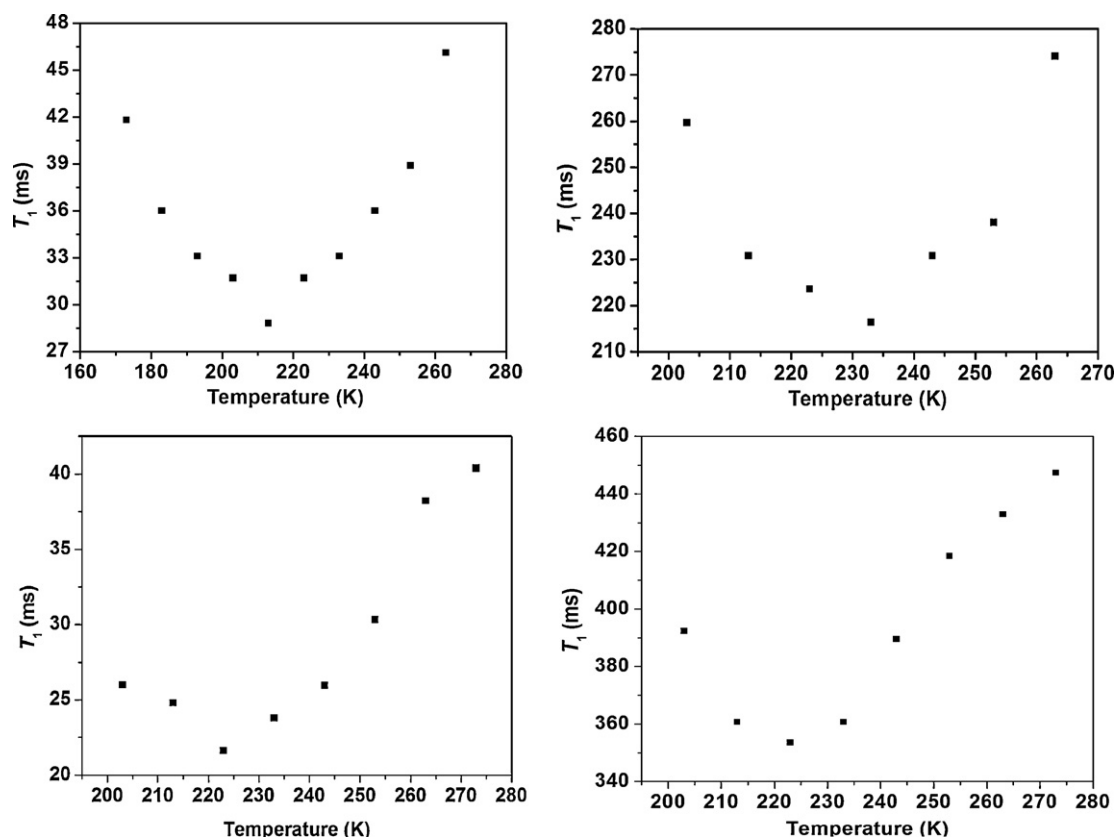


Fig. 13. Plot of  $T_1$  (400 MHz) versus temperature for  $\text{cis-}[\text{Ir}(\text{H})(\eta^2\text{-H}_2)(\eta^2\text{-S}_2\text{CH})(\text{PCy}_3)_2][\text{BF}_4]$  and  $\text{cis-}[\text{Ir}(\text{H})_2(\eta^2\text{-S}_2\text{CH})(\text{PCy}_3)_2]$  (figure was reproduced from Ref. [47], Copyright (2005) American Chemical Society).

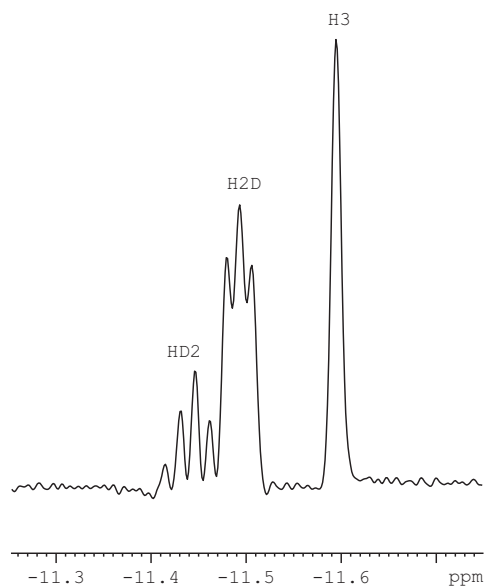
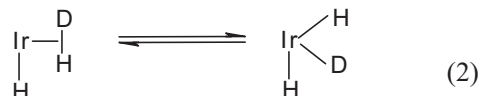
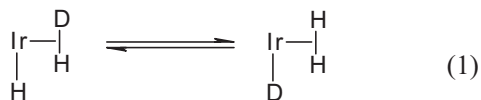


Fig. 14. A plot of hydride region of the  $^1\text{H}$  NMR spectrum of  $15\text{-HD}_2/\text{H}_2\text{D}/\text{H}_3$  (figure was reproduced from Ref. [47], Copyright (2005) American Chemical Society).

attributed to the isotopic perturbation of equilibrium [48] of  $\text{H}_3$ ,  $\text{H}_2\text{D}$  and  $\text{HD}_2$  isotopomers (Scheme 10). Downfield shift for the  $\text{H}_2\text{D}$  and  $\text{HD}_2$  confirmed the occupancy of the deuterium in the hydride site and possibility of trihydride formation may be ruled out on the basis of  $T_1$  and HD coupling.

Chemical shifts and the  $^1J_{\text{HD}}$  data was rigorously analyzed as followed for the hydrotris(pyrozylyl)borate dihydrogen/hydride complexes of Ir and Rh [44] to obtain the limiting chemical shifts and  $^1J_{\text{HD}}$  of the metal bound  $\text{H}_2$ . The limiting chemical shifts obtained for the dihydrogen and the terminal hydride was  $\delta_{\text{H}_2} = -10.58$  ppm and  $\delta_{\text{H}} = -13.61$  ppm. Similar analysis was carried out for a series of dihydrogen-hydride complexes in which deuterium preferred to occupy terminal hydride site [44]. Furthermore, based on the temperature dependent isotope



Scheme 10.  $\text{H}_3$ ,  $\text{H}_2\text{D}$  and  $\text{HD}_2$  in isotopic perturbation of equilibrium [48].

shifts, the isotope perturbation analysis was carried out for a series of iridium complexes of the type  $[\text{Tp}^{\text{R}2}\text{Ir}(\text{L})(\text{H}_2)(\text{H})][\text{BF}_4]$  (Tp = hydrotris(1-pyrazolyl)borate, R = H, L =  $\text{PMe}_3$ ,  $\text{PPh}_3$ , R = Me, L =  $\text{PMe}_3$  and  $[\text{TpRh}(\text{PPh}_3)(\text{H}_2)(\text{H})][\text{B}(\text{Ar})_4]$  (Ar = 3,5-( $\text{CF}_3$ ) $_2\text{C}_6\text{H}_3$ ). For structurally similar ruthenium complexes, Chaudret and co-workers reported trihydride to dihydrogen/hydride transformation upon substitution of cyclopentadienyl (Cp) with hydrotris(1-pyrazolyl)borate (Tp) [49,50]. Tp provides more electron density on the metal center than Cp does, which favored formation of stable trihydride species over dihydrogen/hydride. In contrast, Tp transfers less electron density for the late transition metals which probably due to the poor orbital overlaps with the metal [51].

Since even at low temperature (158 K), the  $^1\text{H}$  NMR limiting chemical shift was not evident for *cis*- $[\text{Ir}(\text{H})(\eta^2\text{-H}_2)(\eta^2\text{-S}_2\text{CH})(\text{PCy}_3)_2][\text{BF}_4]$  **15**; the pre-assumption was that the activation energy for the H atom site exchange ( $\Delta G^\ddagger$ ) must be very low ( $\leq 5 \text{ kcal mole}^{-1}$ ). Heinekey and co-workers obtained similar result ( $\Delta G^\ddagger \leq 5 \text{ kcal mole}^{-1}$ ) for an iridium complex  $[\text{TpIr}(\text{PMe}_3)(\eta^2\text{-H}_2)(\text{H})][\text{BF}_4]$  **10** in which case corresponding limiting chemical shifts of  $\text{M}(\eta^2\text{-H}_2)$  and  $\text{M-H}$  were estimated using the isotope perturbation of resonance [44].

For complex **15**, we considered two distinct dynamic processes: (a) rotation of the  $\text{H}_2$  ligand around the  $\text{M-H}_2$  bond axis since barriers to hydrogen rotation are quite low; (b) the H atom exchange between the dihydrogen and the hydride ligands. The combination of the positive charge and influence of the phosphines could result in heterolysis of  $\text{H}_2$  followed by a proton transfer to the hydride moiety rendering the three hydride ligands equivalent with respect to the NMR time scale. Involvement of an associative type of mechanism to generate a trihydrogen intermediate or transition state could take place in a highly concerted manner which makes the three H's equivalent. Complex *cis*- $[\text{Ir}(\text{H})(\eta^2\text{-H}_2)(\eta^2\text{-S}_2\text{CH})(\text{PCy}_3)_2][\text{BF}_4]$  **15** exhibited considerable elongation of H-H bond as observed for the complexes of the type  $[\text{M}(\text{H})_4(\text{Cp})(\eta^2\text{-H}_2)(\text{PR}_3)]^+$  in which the stretching of H-H toward an adjacent hydride site was a low-energy process leading to a transition state of trihydrogen ( $\text{H}_3$ ) character [54]. The presumed barrier for the exchange process in *cis*- $[\text{Ir}(\text{H})(\eta^2\text{-H}_2)(\eta^2\text{-S}_2\text{CH})(\text{PCy}_3)_2][\text{BF}_4]$  **15** was in agreement with no decoalesce of the  $^1\text{H}$  NMR signal in the hydride region at a temperature 158 K. Similar to our system, estimated low free energy of activation  $\Delta G^\ddagger_{120} \sim 5.5 \text{ kcal mole}^{-1}$  was evident from the decoalesce of  $^{13}\text{C}$  NMR signals of *cis*- $[\text{Ru}(\eta^2\text{-H}_2)(\text{H})(\text{CO})_2(\text{PCy}_3)_2]^+$  **14**. A highly concerted mechanism of the H-atom exchange in a trihydrogen structure was suggested from the spectroscopic evidences [45]. Additionally, rapid H-atom exchange behavior was reported for a series of *ortho*-metalated *cis*-(dihydrogen)-(hydride) complexes **113–115** (Fig. 15) [55,56] in which case exchange couplings between the H and the  $\text{H}_2$  ligands were determined by VT  $^1\text{H}$  NMR (Fig. 15) and DFT at the B3PW91 level [55]. The coherent (quantum mechanical) as well as the incoherent (classical) exchange rates were determined by line shape analysis (ligand:  $E_a(\text{coherent}) = \text{ca. } 10 \text{ kJ mol}^{-1}$ ,  $E_a(\text{incoherent}) = \text{ca. } 40 \text{ kJ mol}^{-1}$  (ca.  $50 \text{ kJ mol}^{-1}$  by DFT at B3PW91 level). Results of these

analysis supported that the activation energy values were independent of the nature of N,C donor aromatic ligand [55,56].

Trihydride or dihydrogen-hydride complexes were preferred candidates for the study of oxidatively induced reductive elimination (OIRE) of  $\text{H}_2$ . The process of oxidatively induced reductive elimination (OIRE) of  $\text{H}_2$  in a trihydride or in a paramagnetic “stretched” dihydrogen complex was studied for  $[\text{Cp}^*\text{Mo}(\text{dppe})\text{H}_3]$  (dppe =  $\text{Ph}_2\text{CH}_2\text{CH}_2\text{PPh}_2$ ) and for the solvent-stabilized product  $[\text{Cp}^*\text{Mo}(\text{dppe})(\text{solv})\text{H}]^+$  by EPR spectroscopy [169]. This was the first structural characterization of the starting and end product, a rare 15-electron hydride complex, of the OIRE process of  $\text{H}_2$ . After this inspiring work, Poli et al. reported new systems  $[\text{Cp}^t\text{BuMo}(\text{PMe}_3)_2\text{H}_3]^+$  and  $[\text{Cp}^t\text{BuMo}(\text{PMe}_3)_2\text{H}]^+$  with strongly donating  $\text{PMe}_3$  and sterically protecting 1,2,4- $\text{C}_5\text{H}_2^t\text{Bu}_3$  ( $\text{Cp}^t\text{Bu}$ ) ligand which allowed to isolate and structurally characterize the starting and end products of the  $\text{H}_2$  OIRE [170]. The X-ray diffraction analysis revealed the identity of the complex  $[\text{Cp}^t\text{BuMo}(\text{PMe}_3)_2\text{H}]^+\text{PF}_6^-$  resulted by  $\text{H}_2$ -elimination (Fig. 16(b)). Its formation from  $[\text{Cp}^t\text{BuMo}(\text{PMe}_3)_2\text{H}_3]^+$  (Fig. 16(a)) can be anticipated as the collapse of the  $\text{H}_2$  and  $\text{H}_3$  atoms (Fig. 16(a)) to yield a putative  $[\text{Cp}^t\text{BuMo}(\text{PMe}_3)_2\text{H}(\text{H}_2)]^+\text{PF}_6^-$  nonclassical intermediate, followed by  $\text{H}_2$  dissociation.

Effect of oxidation on the  $\text{H}_2$  reductive elimination from polyhydrides is also an interesting topic. Sterically protected molybdenum trihydride redox pairs with substituted cyclopentadienyls ( $\text{C}_5\text{H}^t\text{Pr}_4$ , 1,2,4- $\text{C}_5\text{H}_2^t\text{Bu}_3$ ) and  $\text{PMe}_3$  were reported among which a 17-electron oxidation product  $[\text{Mo}(1,2,4\text{-C}_5\text{H}_2^t\text{Bu}_3)(\text{PMe}_3)_2\text{H}_3]^+$  and its subsequent  $\text{H}_2$  elimination process lead to the 15-electron monohydride complex  $[\text{Mo}(1,2,4\text{-C}_5\text{H}_2^t\text{Bu}_3)(\text{PMe}_3)_2\text{H}]^+$  [171]. Sterically protected 17-electron trihydride complexes exhibited a dissociative pathway for  $\text{H}_2$  substitution by a solvent molecule (Scheme 11).

#### 5.4. Coordinately unsaturated dihydrogen complexes

Limited numbers of coordinately unsaturated dihydrogen complexes have been reported. Chaudret and Sabo-Etienne et al. have extensively studied a series of ruthenium based coordinately unsaturated complexes  $\text{RuHX}(\text{H}_2)(\text{PCy}_3)_2$  (X = I, Br, Cl, SCy, S<sup>t</sup>Bu, etc., Fig. 3) [57]. Similar studies revealed that structurally similar osmium complexes  $[\text{Os}(\text{H})_3\text{X}(\text{P}^t\text{Pr}_3)_2]$  (X = Cl **116**, Br **117**, I **118**) exhibited classical trihydric character while possessing a large  $J_{\text{HH}}$ 's with strong exchange couplings and distinct structural features in contrast to the ruthenium series [58]. Sterically influencing phosphine ligands dictated the complexes  $\text{Ru}(\text{H})(\text{X})(\eta^2\text{-H}_2)(\text{P}^t\text{Pr}_3)_2$  (X = I **119**, Cl **120**) to adapt either dihydrogen/hydride or trihydride structure [59,60]. Results of fluxionality analysis of these complexes indicated that all hydrogens (H-atoms) were equivalent at accessible temperatures in standard solvents. An unstable bis-dihydrogen derivative  $\text{Ru}(\text{H})(\text{I})(\text{H}_2)_2(\text{P}^t\text{Pr}_3)_2$  **121** was obtained from  $\text{Ru}(\text{COD})(\text{COT})$  and  $\text{P}^t\text{Pr}_3$  by treating with  $\text{CH}_3\text{I}$  or  $\text{CH}_3\text{Cl}$  under atmospheric pressure of  $\text{H}_2$ . Complex **121** was reacted with  $\text{H}_2$  resulting an unprecedented bis-dihydrogen complex **122** (Scheme 12). All ruthenium derivatives

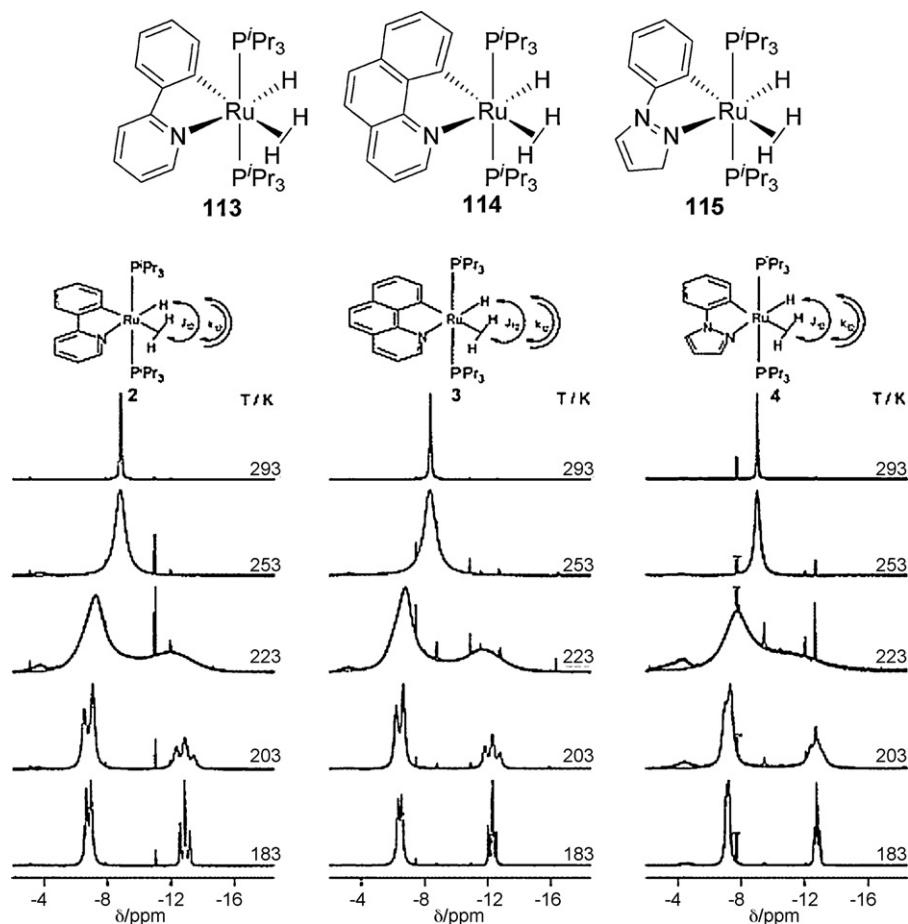


Fig. 15. Structure of ortho-metalated dihydro dihydrogen complexes **113–115** and superimposed experimental and calculated  $^1\text{H}$  NMR (500 MHz) spectra of the hydride region at selected temperature 55 (figure was reproduced from Ref. [55], Copyright (2004) American Chemical Society).

reacted instantaneously with gaseous CO and  $\text{N}_2$  at room temperature to yield two types of dicarbonyl derivatives  $\text{RuH}_2(\text{CO})_2(\text{PCy}_3)_2$  and  $\text{RuHX}(\text{CO})_2(\text{PCy}_3)_2$  ( $\text{X} = \text{I}, \text{Cl}, \text{SCy}, \text{SPh}, \text{S}^t\text{Bu}$ ).

We obtained a 5-coordinated Ru-H<sub>2</sub> complex  $[\text{Ru}(\eta^2\text{-H-H})(\text{PP})_2][\text{OTf}]_2$  ( $\text{PP} = (\text{C}_6\text{H}_5\text{CH}_2)_2\text{PCH}_2\text{CH}_2(\text{CH}_2\text{C}_6\text{H}_5)_2$ ) **17** by the protonation of the corresponding hydride  $[\text{Ru}(\text{H})(\text{PP})_2][\text{OTf}]$  with HOTf (Scheme 13) [31]. Interesting

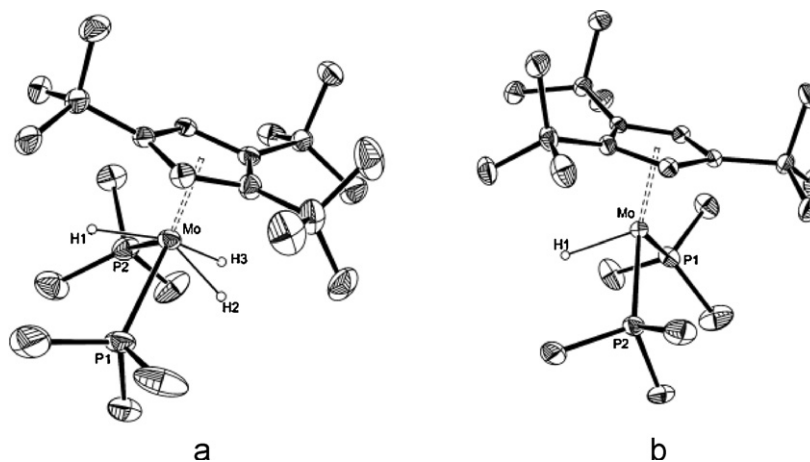
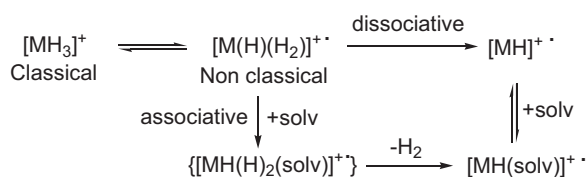
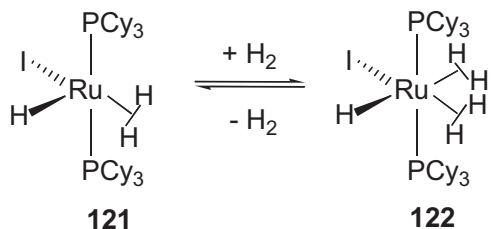


Fig. 16. a: ORTEP view of the cation in  $[\text{Cp}^*\text{BuMo}(\text{PMe}_3)_2\text{H}]\text{PF}_6$  (ellipsoids are drawn at the 30% probability level and all hydrogen atoms except the hydride are omitted for clarity); b: ORTEP views of the cation in  $[\text{Cp}^*\text{BuMo}(\text{PMe}_3)_2\text{H}_3]\text{PF}_6$  (ellipsoids are drawn at the 30% probability level and all hydrogen atoms except the hydrides are omitted for clarity) (figure was reproduced from Ref. [170], Copyright (2007) Wiley-VCH Verlag GmbH & Co. KGaA).



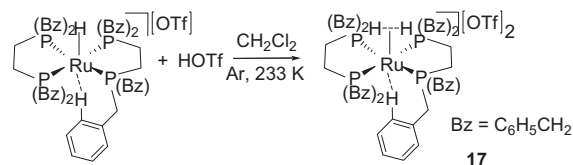
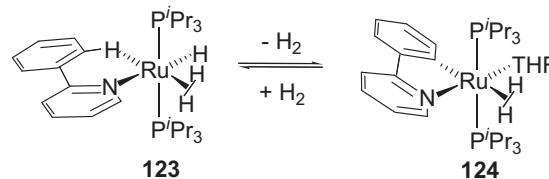
Scheme 11. Oxidation behavior of sterically protected trihydride.

Scheme 12. Reversible binding of H<sub>2</sub> in a coordinately unsaturated dihydrogen complex [60].

to note that the complex **17** was stabilized via agostic interactions through ortho C–H fragment of the phenyl ring *trans* to the metal bound H<sub>2</sub>. To the best of our knowledge, complex **17** contains the longest H–H bond ( $d_{\text{HH}} 1.05 \pm 0.3 \text{ \AA}$  from  $^1J_{\text{HD}}$ ) observed for a *dicationic* Ru–H<sub>2</sub> complex. A limited stability has been noted for **17** which arrest a Cl from solvents like CH<sub>2</sub>Cl<sub>2</sub>, Cl<sub>2</sub>CH<sub>2</sub>CH<sub>2</sub>Cl<sub>2</sub> to result *trans*-dihydrogen-chloride species. A modest temperature variation of  $^1J_{\text{HD}}$  from 22.0 Hz at 293 K to 24.0 Hz at 233 K was recorded similar to the trend observed for many elongated H<sub>2</sub> complexes [8].

Another type of a H<sub>2</sub> complex [Ru(H)X(η<sup>2</sup>-H<sub>2</sub>)(PR<sub>3</sub>)<sub>2</sub>] with a coordinately unsaturated metal center exhibiting a  $d_{\text{HH}} 1.0\text{--}1.03 \text{ \AA}$  was reported [61]. A structurally characterized [Ru(H)(H<sub>2</sub>)(*o*-C<sub>6</sub>H<sub>5</sub>py)(P<sup>i</sup>Pr<sub>3</sub>)<sub>2</sub>][BAR<sup>f</sup>] (BAR<sup>f</sup> = B[C<sub>6</sub>H<sub>3</sub>(CF<sub>3</sub>)<sub>4</sub>]<sub>4</sub>) **123** with significantly shorter H–H distance 0.82 Å contains a Ru...H–C (CH of the phenyl) agostic interaction [61]. This was unprecedented for a metal center accommodating both dihydrogen and a weak agostic interaction existing in equilibrium with resulting species of Ph ortho metallation (Scheme 14). This process of interconversion consists of low activation energy due to the simultaneous presence of hydride and dihydrogen undergoing a classical oxidative addition.

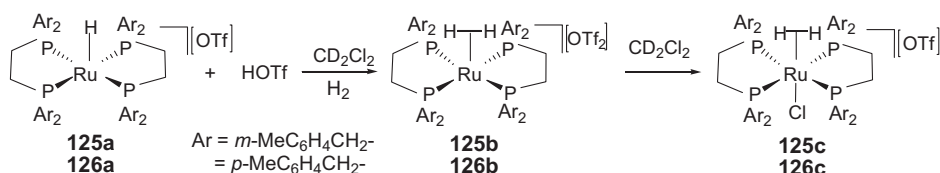
We reported a study on the stability and H...H elongation for a series of coordinately unsaturated complexes [Ru(η<sup>2</sup>-H–H)(PP)<sub>2</sub>][OTf]<sub>2</sub> (PP = (*m*-MeC<sub>6</sub>H<sub>4</sub>CH<sub>2</sub>)<sub>2</sub>PCH<sub>2</sub>CH<sub>2</sub>P(CH<sub>2</sub>C<sub>6</sub>H<sub>4</sub>*m*-Me)<sub>2</sub> **125b**, (*p*-MeC<sub>6</sub>H<sub>4</sub>CH<sub>2</sub>)<sub>2</sub>PCH<sub>2</sub>CH<sub>2</sub>P(CH<sub>2</sub>C<sub>6</sub>H<sub>4</sub>*p*-Me)<sub>2</sub> **126b**) (Scheme 15) [23]. With yet unknown possible reason, unusual H–H elongation

Scheme 13. Formation of a 16-electron dihydrogen complex [Ru(η<sup>2</sup>-H–H)(PP)<sub>2</sub>][OTf]<sub>2</sub> **17** [31].Scheme 14. Reversible binding of H<sub>2</sub> in a dihydrogen complex [61].

( $1.04 \pm 0.001$  and  $1.05 \pm 0.003 \text{ \AA}$ ) was noted for dicationic complexes **125b** and **126b** (Fig. 17) [110].

## 6. Dihydrogen complexes in reversible release of H<sub>2</sub>

Molecular hydrogen is promising to play a central role in new challenges that have emerged in terms of climate change and energy supply. It is widely accepted that the “hydrogen economy” [172] requires breakthroughs in the areas of efficient storage and production of clean hydrogen accompanied with favourable charge/discharge kinetics [62,173]. The widespread use of dihydrogen as an energy carrier for onboard applications is the present challenge for economical and environmental issues [62,174]. Reversible absorption of huge quantities of H<sub>2</sub> and release efficiently under mild conditions is the major requirement for automobile applications by using suitable molecule or material [62,175,176]. Reversibility is an extremely important property which must be the key to the application of the new generation H<sub>2</sub>-storage materials. Reversible uptake of H<sub>2</sub> per molecule is the concerned parameter and the weight percentage for the H<sub>2</sub>-fueling with a design target at 6.5% H<sub>2</sub> by weight is essential [63]. Storage material such as ammonia borane (NH<sub>3</sub>·BH<sub>3</sub>) with 19.6 wt% [177] of H<sub>2</sub> of which a high percentage can easily be released, thus represents a possible vector for the storage and transportation of H<sub>2</sub> [58,63]. Reversible H<sub>2</sub>-releasing systems are thus promising for hydrogen regeneration. To meet the demand, system that performed H<sub>2</sub> uptake reversibly at ambient or near ambient



Scheme 15. Conversion of coordinately unsaturated dihydrogen complexes to dihydrogen-chloride derivative in dichloromethane [23].

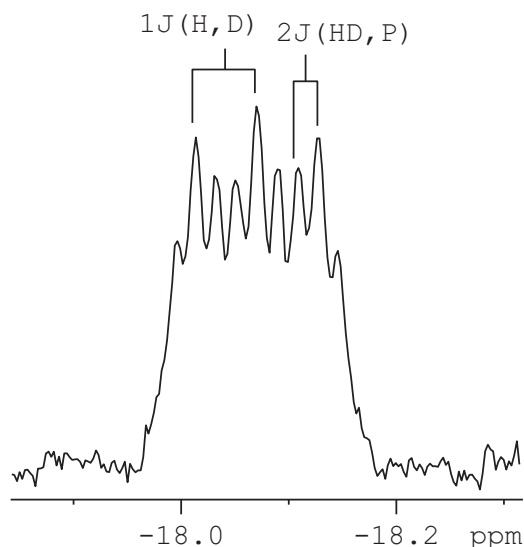
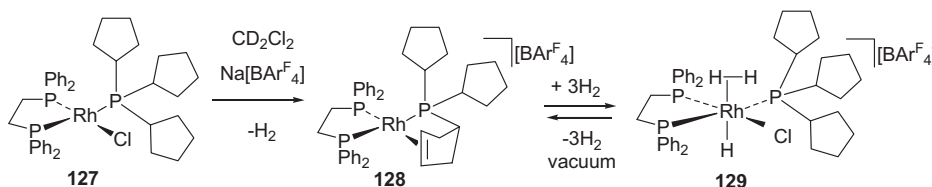
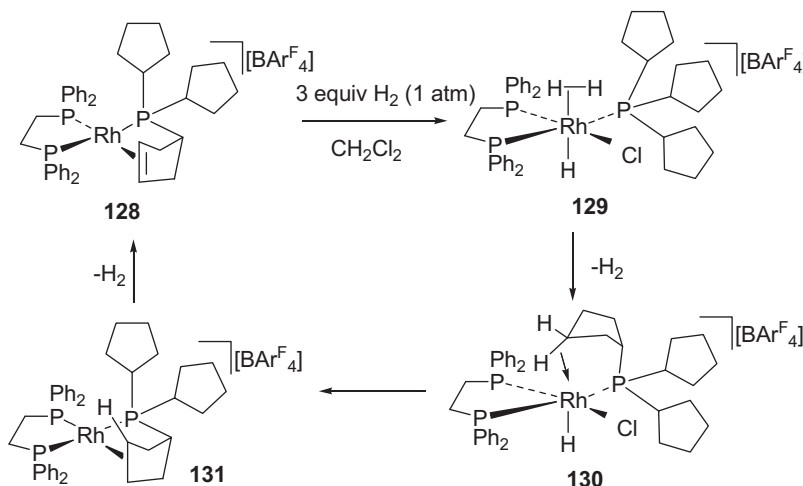


Fig. 17.  $^1\text{H}$  NMR spectrum of the hydride region of  $[\text{Ru}(\eta^2\text{-HD})((p\text{-MeC}_6\text{H}_4\text{CH}_2)_2\text{PCH}_2\text{CH}_2\text{P}(\text{CH}_2\text{C}_6\text{H}_4p\text{-Me})_2)_2][\text{OTf}]_2$  **125b-d<sub>1</sub>**, (figure was reproduced from Ref. [23], Copyright (2008) American Chemical Society).

conditions in the solid-state would be essential [178]. Molecular hydrogen complexes reported by Weller and co-workers showed interesting results. Bis- and tris-cyclopentyl phosphine (PCyp<sub>3</sub>) supported complex  $[\text{Rh}(\text{dppe})\text{Cl}](\text{PCyp}_3)_2$  **127** upon treatment with  $\text{Na}[\text{BAR}_4^{\text{F}}]$ , afforded **128** with hybrid phosphine-olefin donation to



Scheme 16. Reversible release of  $\text{H}_2$  from phosphine supported  $\text{Rh}(\text{I})$  [66].



Scheme 17. Process of reversible  $\text{H}_2$  release from  $\text{Rh}(\text{I})$  [178].

$\text{Rh}(\text{I})$  that upon addition of  $\text{H}_2$  resulted in a hydrogen-dihydride complex  $[\text{Rh}(\text{dppe})(\text{PCyp}_3)(\eta^2\text{-H}_2)(\text{H}_2)][\text{BAR}_4^{\text{F}}]$  **129** (Scheme 16). This operates by a reversible alkyl dehydrogenation process in absence of an  $\text{H}_2$  acceptor in the solid-state to store and release up to three equivalents of  $\text{H}_2$  per cycle [67].

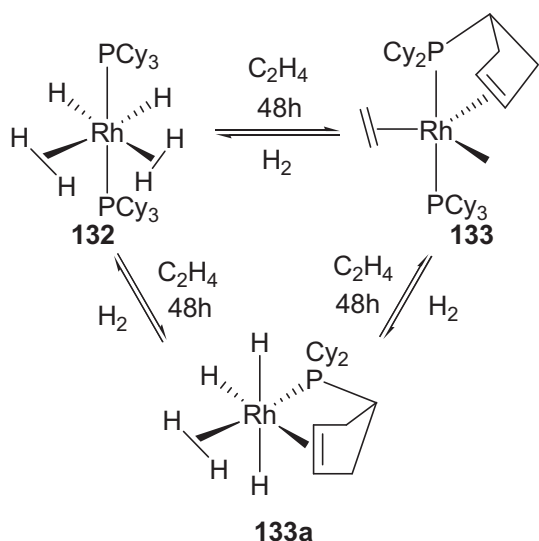
Facile uptake and release up to three equivalents of  $\text{H}_2$  per molecule in the solid state corresponds to a modest  $\text{H}_2$  storage and release of 0.35% (w/w) which was impractical for applications. By placing **128** briefly (seconds) under vacuum at 77 K followed by warming up to room temperature resulted the removal of the bound  $\text{H}_2$  and a fluxional nature of H-atom exchange with an agostic interaction identified by  $^{31}\text{P}\{^1\text{H}\}$  NMR studies (Scheme 17) [179].

A similar phenomena was witnessed for a bis- $\text{H}_2$  complex  $\text{RuH}_2(\eta^2\text{-H}_2)_2(\text{PCyp}_3)_2$  (Cyp = Cyclopentyl) **132** which holds two unstretched  $\text{H}_2$  units ( $d_{\text{HH}} = 0.82\text{--}0.83 \text{ \AA}$  and  $\sim 1.7 \text{ wt\%}$  of the complex) [69]. This reversible process requires an acceptor (ethene) to promote  $\text{H}_2$  release. In this case, a facile and reversible  $\text{H}_2$  release from **132** up to ten hydrogen atoms per molecule was recorded. The reversible dehydrogenation process showed the complete conversion of **133** into the starting complex **132** within 150 min by exposing a  $[\text{D}_{12}]$ cyclohexane solution of **133** to 1 bar pressure of  $\text{H}_2$  at room temperature (Scheme 18).

More recently, a phosphine supported terminal borylene ruthenium complex **134** was found to release  $\text{H}_2$  reversibly at room temperature (Scheme 19) [68].

A solvent and intramolecular interaction dependent  $\text{H}_2$  loss was reported for bis- $\text{H}_2$  complexes in which a





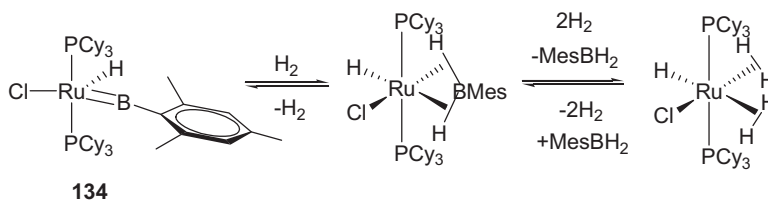
Scheme 18. Reversible dihydrogen release with tricyclopentylphosphine [68].

phosphine facilitates the solvent coordination and CH agostic interaction with the metal center resulting the  $H_2$  loss (Scheme 20) [162].

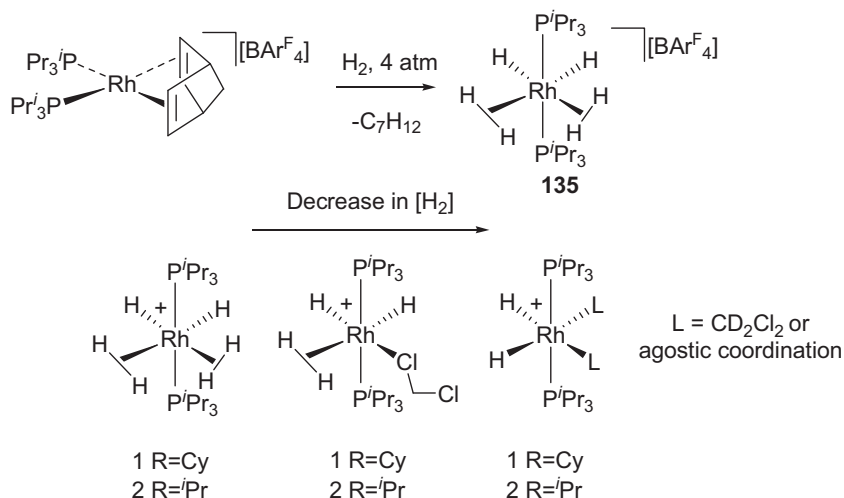
A series of hexarhodium clusters  $[Rh_6(PR_3)_6H_{12}] [BAr^F_4]_2$  ( $R = ^iPr, Cy$ ;  $Ar^F = [B(C_6H_3(CF_3)_2)_4]$ ) [179,162] was obtained from a treatment of  $H_2$  with the complex

$[Rh(H_2)(H)_2(PiPr_3)_2]$  **136** at 4 atm pressure. The rhodium hydrido clusters further reacted with additional two equivalents of the  $H_2$  reversibly (Scheme 21) to result a cluster **138** that holds  $\sim 0.25$  wt% of  $H_2$  at room temperature [180] which does not meet the greater than 6 wt% requirement [181]. For studying the structure and bonding of the hydride clusters, phosphines with sterically congested tri-*t*-butyl substituent can stabilize the coordination unsaturation on the metals and complex would exhibit high reactivity toward  $H_2$  [182]. Clusters which react with  $H_2$  reversibly were useful as molecular model for the reversible attachment of  $H_2$  to a metal center [183,184].

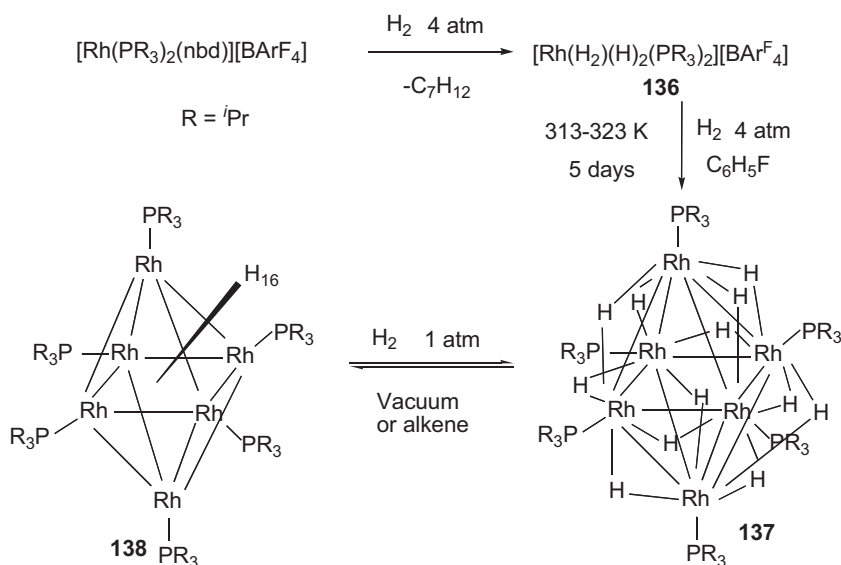
Hydrogen evolutions by molecular catalysts in the context of  $H_2$  production have awakened much apprehension [185]. Of much greater and current interest is the phenomenon of ionic hydrogen activation for catalytic ionic hydrogenation and the reverse process (for solar energy conversion and  $H_2$  production). In this context, dihydrogen bond (DHB) interactions between two metal hydrides that serve as proton acceptor and donor were studied. This was not revealed until the discovery of a DHB adduct of transition-metal hydrides such as nickel(II) pincer complex  $[(^tBuPCP)Ni(H)]$  ( $^tBuPCP = 2,6-C_6H_3(CH_2PtBu_2)_2$ ) **138** and acidic tungsten(II) complex  $[CpW(H)(CO)_3]$  **139** with opposite polarities [186]. Adduct **138**...**139** of two hydride complexes undergoes proton transfer and  $H_2$  evolution. Structural study revealed that the final product was a bimetallic ion paired complex



Scheme 19. Reversible reaction of the borylene complex **134** with  $H_2$  [67].



Scheme 20. A series of bis-dihydrogen complexes lose  $H_2$  on decrease in pressure of  $H_2$  [161].



Scheme 21. Rhodium bis- $\text{H}_2$  complex forming hydrido clusters and reversible release of  $\text{H}_2$  [179].

$[\text{CpW}(\text{CO})_2(\mu-\kappa, \text{C}:\kappa, \text{O}-\text{CO})\cdots\text{Ni}(\text{tBuPCP})]$  **140** (Scheme 22). VT NMR and VT IR spectroscopic studies at 190–298 K confirmed the formation of strong adduct followed by the  $\text{H}_2$  elimination that yielded complex **140**. Interestingly, VT proton spin-lattice relaxation times ( $T_1$ ) of the hydride resonances in  $\text{THF}-d_8$  revealed that **138**–**139** has shorter  $T_1$  than that of **138**. This might be due to the presence of additional dipolar contribution consistent with the formation of a  $\text{NiH}\cdots\text{HW}$  unconventional hydrogen bond which ultimately resulted evolution of  $\text{H}_2$ . At higher temperatures, the resonances caused by complexes **138** and **139** disappeared while **140** resulted together with release of  $\text{H}_2$ . This unconventional  $\text{H}\cdots\text{H}$  interaction followed by  $\text{H}_2$  evolution has relevance for efficient  $\text{H}_2$  production.

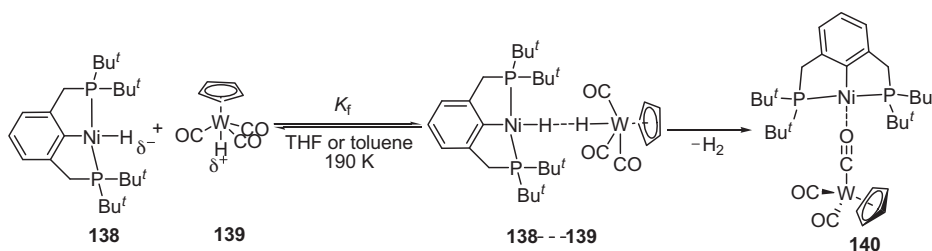
DFT calculations at the M06 level supported the formation of an intermediate adduct (**138**–**139**) by the interaction of two complexes through their hydrides and cyclopentadienyl C–H bond. DFT results can also be interpreted as the adduct **138**–**139** containing a “bridging nonclassical dihydrogen ligand” [186]. It has been considered that an elongated  $\text{H}_2$  connects two metal centers in an unusual  $\mu, \eta^{1:1}$  end-on mode.

Proton transfer involving transition metal hydrides and/or heterolytic splitting of H–H bond are important steps in catalytic processes, including ionic hydrogenation and reduction of  $\text{H}^+$  or  $\text{H}_2$ . Kinetic and thermodynamic

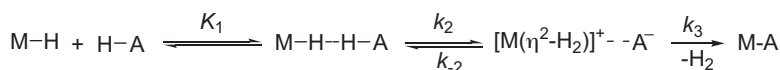
parameters,  $\text{MH}\cdots\text{HA}$  proton transfer, subsequent  $\text{H}_2$  evolution and factors determining the stability of  $\text{MH}\cdots\text{HA}\cdots\text{HA}$  adduct have been major concerns [187]. It was postulated that the proton transfer process is rate-determining step for this  $\text{H}_2$  evolution process. Thus it can be represented as represented in Scheme 23 with  $k_3 \gg k_{-2}$  and for the rate constant  $k_{\text{obs}}$  transforms into  $k_2$ .

Fine-tuning of the  $[\text{M}(\eta^2\text{-H}_2)]^+[\text{A}]^-$  ion pair can provide additional support in governing the reactivity of the non-classical hydride species. It appears that the nature of the solvent and the amount of excess acid determine the reaction product by delicately controlling the proton transfer and ion pairing equilibria between  $[\text{Cp}^*\text{MoH}_3(\text{dppe})]$  and  $[\text{CF}_3\text{COOH}]$  (Scheme 24) [188]. The use of suitable solvent and hydride/acid ratio led to the selective formation of the dihydrido complex  $[\text{Cp}^*\text{Mo}(\text{dppe})(\text{H})_2(\eta^1\text{-O}_2\text{CCF}_3)]$  as  $\text{H}_2$  elimination product. The  $[\text{Cp}^*\text{MoH}_4(\text{dppe})]^+\cdots[\text{OCOCF}_3]^-$  ion pair dissociation precludes the formation of the trifluoroacetate leading to the non-specific  $\text{H}_2$  loss/decomposition (Scheme 24).

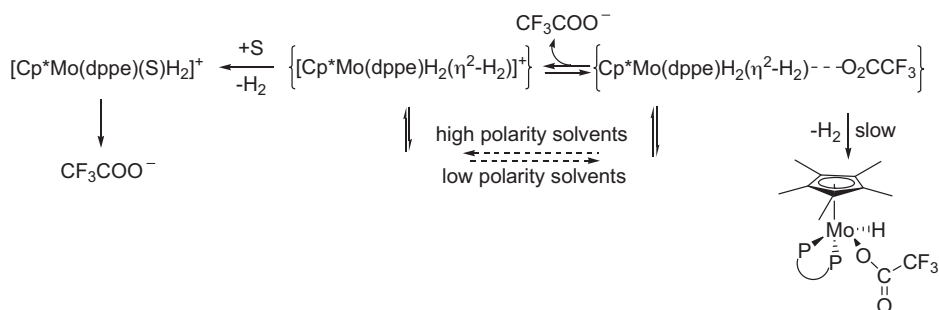
Photolysis of  $\text{M}(\text{CO})_6$  ( $\text{M} = \text{Cr}, \text{W}$ ) at low temperature in the presence of hydrogen gas afforded dihydrogen complexes  $\text{Cr}(\text{CO})_5(\text{H}_2)$  and  $\text{W}(\text{CO})_5(\text{H}_2)$  exhibiting short  $T_1$  values for the hydride resonances and large HD coupling for HD isotopomer [189]. Photochemical generation of  $\text{H}_2$  complexes was also successful by irradiating the



Scheme 22. Reaction between metal hydrides **138** and **139**.



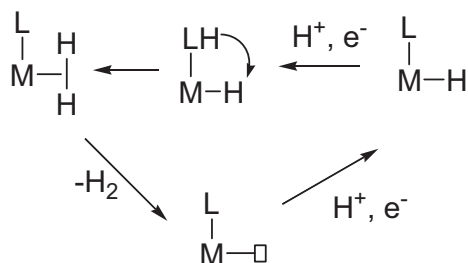
Scheme 23. Kinetic model for the reaction of two metal hydrides toward H<sub>2</sub> evolution via H...H interaction.



Scheme 24. Proton transfer and ion-pairing equilibria.

phosphine-substituted derivatives (PMe<sub>3</sub>)Cr(CO)<sub>5</sub> and (PMe<sub>3</sub>)W(CO)<sub>5</sub> in the presence of H<sub>2</sub> gas resulting *cis*-(PMe<sub>3</sub>)Cr(CO)<sub>4</sub>(H<sub>2</sub>) and *trans*-(PMe<sub>3</sub>)Cr(CO)<sub>4</sub>(H<sub>2</sub>) in CH<sub>2</sub>Cl<sub>2</sub>. In this process, solvent binding was found to be competitive with that of H<sub>2</sub>. Photochemically generated H<sub>2</sub> complexes can be deprotonated by mild bases. Analysis of *T*<sub>1min</sub> data for the dihydrogen complexes lead to *d*<sub>HH</sub> = 0.86–0.87 Å for slow H<sub>2</sub> rotation. Corresponding short *d*<sub>HH</sub> values were consistent with relatively weak interaction of H<sub>2</sub> and the metal center. Photochemically assisted facile formation of CO-rich Cr and W dihydrogen complexes in conventional solvents with weak H<sub>2</sub> binding was dependent on the donor ability of the trans ligand. In this case, H–H bond elongation to a negligible extent was possible but a heterolytic activation evident due to the influence of PMe<sub>3</sub>. Photochemically generated complexes with weak bonding with H<sub>2</sub> might be relevant for the photochemical H<sub>2</sub> generation from other systems.

Nature has invented the process of storing the energy in the chemical form (solar energy conversion) in H<sub>2</sub>. In this process, metabolism through hydrogenase (H<sub>2</sub>ase) acted as catalyst to operate reversible oxidation of H<sub>2</sub> to protons and electrons [190–193]. In concerning to the concept that water must be the source of H<sub>2</sub>, rather than its current production from natural gas, schemes involving use of solar energy to split water are currently of high interest [194–196]. The fundamental features of H<sub>2</sub> production via bioinspired water splitting and other related processes are



Scheme 25. Intramolecular heterolytic splitting and H<sub>2</sub> evolution.

based on the stepwise combination of protons and electrons on a metal center to form a labile H<sub>2</sub>. This “H<sub>2</sub>-evolving module” (Scheme 25) often assisted by proton relays such as in [FeFe]-H<sub>2</sub>ases [197]. This is essentially the microscopic reverse of intramolecular heterolytic splitting of H<sub>2</sub>.

Now there are dozens of schemes to produce H<sub>2</sub> using molecular photocatalysis [195]. Although bimetallic systems have been the focus of the most straightforward efforts to model H<sub>2</sub>ase function, monometallic complexes also activate H<sub>2</sub> and function as electrocatalysts for H<sub>2</sub> splitting/production. For example, a phosphine bound Ni system (Fig. 18) was covalently attached onto multiwalled carbon nanotubes in a high surface area cathode material by Le Goff et al. [198]. The pendant nitrogen acted as the proton relay in which surface immobilization of the catalyst allows operation under the aqueous conditions crucial for using such catalysts in proton-exchange membrane (PEM) electrolyzers and fuel cells. The catalyst operated under conditions comparable to those encountered in PEM devices and demonstrated sustained performance for both the production (> 100,000 turnovers, or cycles of the reaction) and oxidation (> 35,000 turnovers) of H<sub>2</sub>.

There were many attempts to construct monomolecular and biomolecular devices for photohydrogen production. For example, electrons could be supplied to a [FeFe]-H<sub>2</sub>ase model by a photochemical module: e.g., the well-known Ru(bipy)<sub>3</sub> system, studied by Sun, Ott, and Artero et al. [199]. A suitable process for building molecular photocatalysts is to anchor a sensitizer to the model of [FeFe]-H<sub>2</sub>ases active site for H<sub>2</sub> generation using visible light [200]. Following the strategies of dithiolate-bridge connector between sensitizer and [FeFe]-H<sub>2</sub>ases and anchoring the sensitizer to one of the iron centers of the [FeFe]-H<sub>2</sub>ases, several covalently linked systems of sensitizer-[FeFe]-H<sub>2</sub>ases active site were constructed. However, examples of photochemically driven proton-reduction systems using molecular H<sub>2</sub>ases mimics as catalysts for H<sub>2</sub> evolution were hardly known. Electrochemical and photophysical studies suggested that the more negative

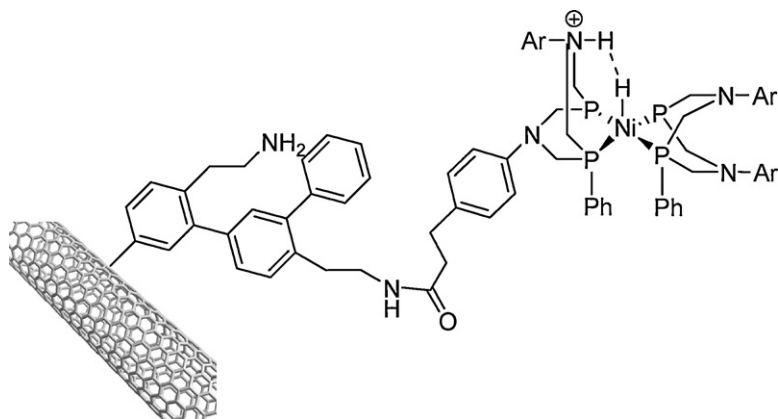
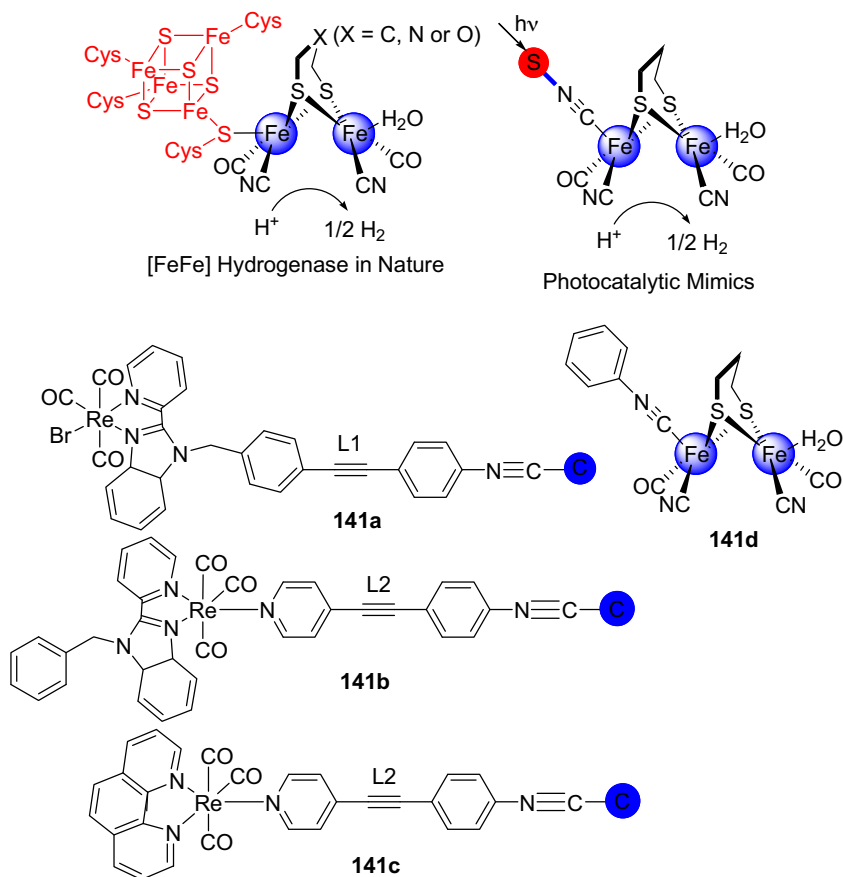


Fig. 18. Ni-P complex attached to multiwalled carbon nanotubes in a high-surface area cathode material [198].

potential of the active site of [FeFe]-H<sub>2</sub>ases with respect to the excited state reduction potential of Ru<sup>II</sup> sensitizer renders the photo-reduction of the [FeFe]-H<sub>2</sub>ases active site thermodynamically unfeasible, leading to intramolecular photochemical H<sub>2</sub> production rather challenging [201]. To mimic [FeFe] hydrogenase (H<sub>2</sub>ases), many molecular photocatalysts were designed among which systems **141a**, **141b**, and **141c**, mimics the photocatalytic

H<sub>2</sub> evolution at room temperature (Scheme 26). Rhenium(I) complex was considered as photosensitizer **S** owing to its visible-light absorption, long excited-state lifetime, more negative excited state reduction potential, thermal and photochemical stability. An active site model of [μ-S<sub>2</sub>(CH<sub>2</sub>)<sub>3</sub>][Fe<sub>2</sub>(CO)<sub>5</sub>CN] was utilized as a catalytic reaction center **C**. A cyanide (CN) group, which is one of the most distinctive features of H<sub>2</sub>ases in nature, was



Scheme 26. [FeFe] Hydrogenase in nature, [FeFe] hydrogenase mimics.

incorporated in the bridge (L) to easily anchor the rhenium(I) **S** to the iron core of Fe<sub>2</sub>S<sub>2</sub> catalytic center **C**. Experimental studies indicated that the amount of H<sub>2</sub> evolution increased in the first 60 min and further irradiation can lead to the decomposition of the catalysts, and thus slows down the rate of H<sub>2</sub> evolution.

Time-dependence of H<sub>2</sub> evolution and spectroscopic study demonstrated that the orientation of **S** and the specific bridge in **141a**, **141b**, and **141c** were important both for the forward electron-transfer step from the excited S\* to the catalytic **C** and the reverse electron-transfer step of the charge-recombination (S<sup>+</sup>-C<sup>-</sup>). It was observed that in terms of steady-state and time-resolved techniques, forward electron-transfer step was much faster, but the reverse electron-transfer step of the charge-recombination was slower, which reminisces the behavior of [FeFe]-H<sub>2</sub>ases in nature [202].

## 7. Conclusion

This review on the properties of metal-H<sub>2</sub> complexes supported by the phosphines has led to conclude that a large number of electronically fine-tuned metal-H<sub>2</sub> complexes and their solution dynamic studies can construct the reaction coordinate for the oxidative addition of H<sub>2</sub> to a metal center. As discussed herein, experimental and theoretical results of metal-H<sub>2</sub> complexes elucidated many facts like elongation of H-H bond to a metal center, H atom site exchange dynamics, and possibility of applying some of these compounds for reversible release of H<sub>2</sub>. Features of metal-H<sub>2</sub> complexes described herein have specifically focused only on the phosphine supported complexes and the salient conclusions of this article are as follows:

1. Properties such as metal-H<sub>2</sub> bonding and the fate of the H-H bonding upon bound to the metal center of metal-H<sub>2</sub> complexes with electron donor monodentate and bidentate phosphines were discussed. Tendency of the various metal ions in forming H<sub>2</sub> complexes and role of the phosphine in stabilizing such species were the focus of the discussion. Based on the experimental and theoretical results, it can be concluded that, in most cases, electronics of the phosphine plays the major role in stabilizing M-H<sub>2</sub> 2e-3c bonding.
2. What should be the amount of electron density on the metal center upon elongation of H...H bond in a metal-H<sub>2</sub> complex; this important question can be addressed from the discussion on the extensive spectroscopic investigations and structure determination of elongated H<sub>2</sub> complexes.
3. Tracking the dynamics of the H-atom site exchange for the complexes with *cis*-M(H)(H<sub>2</sub>) unit elucidated the mechanism of exchange.
4. Discussion on the reversible H<sub>2</sub> release from specially designed H<sub>2</sub> complexes highlighted the possibility of these compounds to be applied for new technology related to the reversible release of H<sub>2</sub>.

Overall, features of the metal-H<sub>2</sub> complexes discussed in this article may attract researchers for developing new systems which can be useful in terms of studying the

factors controlling the H...H elongation, developing efficient catalysts for using in mild conditions, and very important feature like improvement in reversible H<sub>2</sub> release.

Further work is in progress, dealing with the chemistry of osmium dihydrogen complexes incorporating bisphosphine and  $\sigma$ - $\eta^2$ -H<sub>2</sub> because they appear to be interesting targets for the construction of reaction coordinate of the oxidative addition of H<sub>2</sub> to a metal center. We are also investigating on the H<sub>2</sub> release properties of some of the metal-H<sub>2</sub> complexes stable in solid state. To this end, we anticipate that the various features of the metal-H<sub>2</sub> complexes should continue to give new observations and challenges both at the fundamental level and for applications.

## Acknowledgements

I wish to thank all the researchers whose innovative contributions have enriched the research on transition metal-dihydrogen chemistry. I thank the Department of Science & Technology (DST), India, with gratitude for financial support. I also thank the DST, India, for funding the procurement of the X-ray diffractometer and a 400 MHz NMR spectrometer under the "FIST" grant. I gratefully acknowledge Professor Balaji Jagirdar for his suggestive comments on many experiments. I am grateful to the Indian Institute of Science, Bangalore and University of Delhi, Delhi, India for providing the laboratory facilities. I thank University Grant Commission (UGC), India for a DS Kothari "Postdoctoral" Research Grant.

## References

- [1] G.J. Kubas, R.R. Ryan, B.I. Swanson, P.J. Vergamini, H.J. Wasserman, *J. Am. Chem. Soc.* 106 (1984) 451.
- [2] G.J. Kubas, G.C.J. Unkefer, B.I. Swanson, E. Fukushima, *J. Am. Chem. Soc.* 108 (1986) 7000.
- [3] G.J. Kubas, *Acc. Chem. Res.* 21 (1988) 120.
- [4] G.J. Kubas, *Metal Dihydrogen and  $\sigma$ -Bond Complexes*, Kluwer Academic/Plenum Publishers, New York, 2001.
- [5] P.G. Jessop, R.H. Morris, *Coord. Chem. Rev.* 121 (1992) 155.
- [6] R.H. Crabtree, *Acc. Chem. Res.* 23 (1990) 95.
- [7] D.M. Heinekey, W.J. Oldham Jr., *Chem. Rev.* 93 (1993) 913.
- [8] D.M. Heinekey, A. Liedós, A.J.M. Lluch, *Chem. Soc. Rev.* 33 (2004) 175.
- [9] S. Sabo-Étienne, B. Chaudret, *Coord. Chem. Rev.* 178-180 (1998) 381.
- [10] L. Torres, R. Gelabert, *J. Chem. Phys.* 117 (2002) 7094.
- [11] R. Gelabert, M. Moreno, J.M. Lluch, *Chem. Eur. J.* 11 (2005) 6315.
- [12] R. Gelabert, M. Moreno, J.M. Lluch, A. Lledos, *Chem. Phys.* 241 (1999) 155.
- [13] G. Barea, M.A. Esteruelas, A. Lledos, A.N. Lopez, J. Tolosa, *Inorg. Chem.* 37 (1998) 5033.
- [14] R. Gelabert, M. Moreno, J.M. Lluch, A. Lledos, *J. Am. Chem. Soc.* 120 (1998) 8168.
- [15] M. Yousufuddin, T.B. Web, S.A. Mason, G.J. McIntyre, G. Jia, R. Bau, *Angew. Chem. Int. Ed. Engl.* 44 (2005) 7227.
- [16] W.T. Klooster, T.F. Koetzle, F. Thomas, G. Jia, T.P. Fong, R.H. Morris, *J. Am. Chem. Soc.* 116 (1994) 7677.
- [17] C.L. Gross, D.M. Young, A.J. Schultz, G.S. Gerolami, *J. Chem. Soc. Dalton Trans.* (1997) 3081.
- [18] V. Pons, M.D. Heinekey, *J. Am. Chem. Soc.* 125 (2003) 8428.
- [19] J.K. Laws, H. Mellows, M.D. Heinekey, *J. Am. Chem. Soc.* 124 (2002) 1024.
- [20] J.K. Laws, H. Mellows, M.D. Heinekey, *J. Am. Chem. Soc.* 123 (2001) 2085.
- [21] P. Barrio, M.A. Esteruelas, A. Lledos, E. Onate, J. Tomas, *Organometallics* 23 (2004) 3008.
- [22] P. Barrio, M.A. Esteruelas, E. Onate, *Organometallics* 21 (2002) 2491.
- [23] S. Dutta, B.R. Jagirdar, M. Nethaji, *Inorg. Chem.* 47 (2008) 547.



- [24] R. Gelabert, M. Moreno, J.M. Lluch, A. Lledós, *J. Am. Chem. Soc.* 119 (1997) 9840.
- [25] D. Gusev, G.S. Llamazares, H. Jacobsen, H. Berke, *Organometallics* 18 (1999) 75.
- [26] F.A. Jalón, A. Otero, B.R. Manzano, E. Villaseñor, B. Chaudret, *J. Am. Chem. Soc.* 117 (1995) 10123.
- [27] G. Barea, M.A. Esteruelas, A. Lledós, A.M. López, E. Oñate, J.I. Tolosa, *Organometallics* 17 (1998) 4065.
- [28] G. Ferrando, K.G. Caulton, *Inorg. Chem.* 38 (1999) 4168.
- [29] J.C. Light, I.P. Hamilton, J.V.J. Lill, *Chem. Phys.* 82 (1885) 1400.
- [30] D.T. Colbert, W.H.J. Miller, *Chem. Phys.* 96 (1992) 1982.
- [31] S. Dutta, B.R. Jagirdar, *Inorg. Chem.* 45 (2006) 7047.
- [32] P. Barrio, M.A. Esteruelas, A. Lledós, E. Oñate, J. Tomàs, *Organometallics* 23 (2004) 3008.
- [33] B. Eguillor, M.A. Esteruelas, M. Oliván, *Organometallics* 25 (2006) 4691.
- [34] P. Barrio, M.A. Esteruelas, E. Oñate, *Organometallics* 21 (2002) 2491.
- [35] P. Barrio, M.A. Esteruelas, E. Oñate, *Organometallics* 22 (2003) 2472.
- [36] M.L. Buil, M.A. Esteruelas, K. Garcés, M. Oliván, E. Oñate, *Organometallics* 27 (2008) 4680.
- [37] G.G. Hlatky, R.H. Crabtree, *Coord. Chem. Rev.* 65 (1985) 1.
- [38] S. Sabo-Etienne, B. Chaudret, *Chem. Rev.* 98 (1998) 2077.
- [39] Z. Lin, M.B. Hall, *Coord. Chem. Rev.* 135/136 (1994) 845.
- [40] R.H. Crabtree, *Angew. Chem. Int. Ed. Engl.* 32 (1993) 789.
- [41] M.A. Esteruelas, L.A. Oro, *Chem. Rev.* 98 (1998) 577.
- [42] R.H. Crabtree, M. Lavin, L. Bonnevot, *J. Am. Chem. Soc.* 108 (1986) 4032.
- [43] N. Bampos, D.L. Field, *Inorg. Chem.* 29 (1990) 587.
- [44] W.J. Oldham, S. Hinkle, S. Amber Jr., D.M. Heinekey, *J. Am. Chem. Soc.* 119 (1997) 11028.
- [45] D.M. Heinekey, H. Mellows, T. Pratun, *J. Am. Chem. Soc.* 122 (2000) 6498, and references therein.
- [46] T.L. Felicia, M. Heather, S. Peter, P.J. White, F.J. Hollander, R.G. Bergman, M. Brookhart, D.M. Heinekey, *J. Am. Chem. Soc.* 124 (2002) 5100.
- [47] H.V. Nanishankar, S. Dutta, M. Nethaji, B.R. Jagirdar, *Inorg. Chem.* 44 (2005) 6203.
- [48] M. Saunders, R.M. Kates, *J. Am. Chem. Soc.* 90 (1977) 8070.
- [49] B. Moreno, S. Sabo-Etienne, B. Chaudret, A. Rodriguez-Fernandez, F. Jalón, S. Trofimenko, *J. Am. Chem. Soc.* 116 (1994) 2635.
- [50] B. Moreno, S. Sabo-Etienne, B. Chaudret, A. Rodriguez-Fernandez, F. Jalón, S. Trofimenko, *J. Am. Chem. Soc.* 117 (1994) 7441.
- [51] P.L. Szajek, J.R. Lawson, R.J. Shapley, *Organometallics* 10 (1991) 357.
- [52] A.F. Jalón, A. Otero, R.B. Manzano, E. Villaseñor, B. Chaudret, *J. Am. Chem. Soc.* 117 (1995) 10123.
- [53] S. Sabo-Etienne, B. Chaudret, A.H. el Makarim, J. Bartlet, J. Daudey, S. Ulrich, H. Limbach, C. Moise, *J. Am. Chem. Soc.* 117 (1995) 11602.
- [54] A.C. Bayse, B.M. Hall, B. Pleune, R. Poli, *Organometallics* 17 (1998) 4309.
- [55] J. Matthes, S. Gründemann, A. Toner, Y. Guari, B. Donnadiou, J. Spandl, S. Sabo-Etienne, E. Clot, H.H. Limbach, B. Chaudret, *Organometallics* 23 (2004) 1424.
- [56] A. Tonner, J. Matthes, S. Gründemann, H.H. Limbach, B. Chaudret, E. Clot, S. Sabo-Etienne, *Proc. Natl. Acad. Sci. U S A* 104 (2007) 6945.
- [57] M. Lorraine, S. Sabo-Etienne, B. Chaudret, *Organometallics* 13 (1994) 3800.
- [58] D.G. Gusev, R. Kulhman, G. Sini, O. Eisenstein, K.G. Caulton, *J. Am. Chem. Soc.* 116 (1994) 2685.
- [59] T. Burrow, S. Sabo-Etienne, B. Chaudret, *Inorg. Chem.* 34 (1995) 2470.
- [60] B. Chaudret, G. Chung, O. Eisenstein, A.S. Jackson, F. Lahoz, J. Lopez, *J. Am. Chem. Soc.* 113 (1991) 2314.
- [61] A.J. Tonner, S. Gründemann, E. Clot, H. Limbach, B. Donnadiou, S. Sabo-Etienne, B. Chaudret, *J. Am. Chem. Soc.* 122 (2000) 6777.
- [62] L. Schlapbach, A. Züttel, *Nature* 414 (2001) 353.
- [63] N.L. Rosi, J. Eckert, M. Eddaoudi, D.T. Vodak, M. O'Keer, O.M. Yaghi, *Science* 300 (2003) 1127.
- [64] X. Zhao, B. Xiao, A.J. Fletcher, K.M. Thomas, D. Bradshaw, M.J. Rosinsky, *Science* 306 (2004) 1012.
- [65] S. Satyapal, J. Petrovic, C. Read, G. Thomas, G. Ordaz, *Catal. Today* 120 (2007) 246.
- [66] F.H. Stephens, V. Pons, R.T. Baker, *Dalton Trans.* (2007) 2613.
- [67] T.M. Douglas, A.S. Weller, *New J. Chem.* 32 (2008) 966.
- [68] G. Alcaraz, U. Helmstedt, E. Clot, L. Vendier, S. Sabo-Etienne, *J. Am. Chem. Soc.* 130 (2008) 12878.
- [69] M. Grellier, L. Vendier, S. Sabo-Etienne, *Angew. Chem. Int. Ed. Engl.* 46 (2007) 2613.
- [70] CRC Handbook of Chemistry and Physics, 87th Ed. Taylor and Francis, 2006–2007, Section 9, p. 22 and p. 57.
- [71] G.J. Kubas, *Chem. Commun.* (1980) 61.
- [72] H.J. Wasserman, G.J. Kubas, R.R. Ryan, *J. Am. Chem. Soc.* 108 (1986) 2294.
- [73] R.H. Crabtree, D.G. Hamilton, *J. Am. Chem. Soc.* 108 (1986) 3124.
- [74] P.J. Brothers, *Prog. Inorg. Chem.* 28 (1981) 1.
- [75] A.M. Joshi, B.R. James, *J. Chem. Soc. Chem. Commun.* (1989) 1785.
- [76] C. Bianchini, A. Meli, M. Peruzzini, P. Frediani, C. Bohanna, M.A. Esteruelas, L.A. Oro, *Organometallics* 11 (1992) 138.
- [77] A. Vigalok, Y. Ben-David, D. Milstein, *Organometallics* 15 (1996) 1839.
- [78] R.M. Bullock, B.J. Rappoli, *J. Am. Chem. Soc.* 122 (2000) 12594.
- [79] H. guan, M. Limura, M.P. Magee, J.R. Norton, G. Zhu, *J. Am. Chem. Soc.* 127 (2005) 7805.
- [80] Y. Nishibayashi, I. Takei, M. Hidai, *Angew. Chem. Int. Ed. Engl.* 38 (1999) 3047.
- [81] T. Okhkuma, R. Noyori, *J. Am. Chem. Soc.* 125 (2003) 13490.
- [82] R. Hartman, P. Chen, *Angew. Chem. Int. Ed. Engl.* 40 (2001) 3581.
- [83] K. Abdur-Rashid, E.E. Clapham, A. Hadzovic, J.N. Harvey, A.J. Lough, R.H. Morris, *J. Am. Chem. Soc.* 124 (2002) 15104.
- [84] C.P. Casey, J.B. Johnson, S.W. Sunger, Q. Cui, *J. Am. Chem. Soc.* 127 (2005) 3100.
- [85] R. Abble, K. Abdur-Rashid, M. Faatz, A. Hadzovic, A.J. Lough, R.H. Morris, *J. Am. Chem. Soc.* 127 (2005) 1870.
- [86] B. Chan, L. Random, *J. Am. Chem. Soc.* 127 (2005) 2443.
- [87] S.E. Clapham, A. Hadzovic, R.H. Morris, *Coord. Chem. Rev.* 248 (2004) 2201.
- [88] M.P. Magee, J.R. Norton, *J. Am. Chem. Soc.* 123 (2001) 1778.
- [89] M.A. Esteruelas, L.A. Oro, C. Valero, *Organometallics* 10 (1991) 462.
- [90] E.G. Lundquist, K. Folting, W.E. Stereib, J.C. Huffman, O. Eisenstein, K.G. Caulton, *J. Am. Chem. Soc.* 112 (1990) 855.
- [91] D.E. Linn, J. Halpern, *J. Am. Chem. Soc.* 109 (1987) 2969.
- [92] A.F. Borowski, S. Sabo-Etienne, B. Donnadiou, B. Chaudret, *Organometallics* 22 (2003) 4803.
- [93] M. Hidai, Y. Nishibayashi, in: M. Peruzzini, R. Poli (Eds.), *Recent advances in hydride chemistry*, Elsevier, Amsterdam, 2001.
- [94] R.H. Crabtree, *The organometallic chemistry of the transition metals*, 4th ed., Wiley, New York, 2005, Chapter 9.
- [95] C.P. Lau, S.M. Ng, G. Jia, Z. Lin, *Coord. Chem. Rev.* 251 (2007) 2223.
- [96] W.C. Chan, C.P. Lau, Y.Z. Chen, Y.Q. Fang, S.M. Ng, G. Jia, *Organometallics* 16 (1997) 34.
- [97] G.J. Kubas, *Catal. Lett.* 104 (2005) 79.
- [98] M.H.G. Precht, M. Hölscher, Y. Ben-David, N. Theyssen, R. Loschen, D. Milstein, W. Leitner, *Angew. Chem. Int. Ed. Engl.* 46 (2007) 2269.
- [99] A.C. Albeniz, D.M. Heinekey, R.H. Crabtree, *Inorg. Chem.* 30 (1991) 3632.
- [100] M. Mediat, G.N. tachibana, C.M. Jensen, *Inorg. Chem.* 31 (1992) 1827.
- [101] D. Giunta, M. Hölscher, C.W. Lehmann, R. Mynott, C. Wirtz, W. Leitner, *Adv. Synth. Catal.* 345 (2003) 1139.
- [102] R. Koelliker, D. Milstein, *J. Am. Chem. Soc.* 113 (1991) 8524.
- [103] F. Maseras, A. Lledós, *Organometallics* 15 (1996) 1218.
- [104] M.A. Esteruelas, J. Herrero, L.A. Oro, *Organometallics* 12 (1993) 2377.
- [105] Y. Kawanami, Y. Sonoda, T. Mori, K. Yamamoto, *Org. Lett.* 4 (2002) 2825.
- [106] A.F. Borowski, S. Sabo-Etienne, M.L. Christ, B. Donnadiou, B. Chaudret, *Organometallics* 15 (1996) 1427.
- [107] Y. Guari, S. Sabo-Etienne, B. Chaudret, *J. Am. Chem. Soc.* 120 (1998) 4228.
- [108] Y. Guari, A. Castellanos, S. Sabo-Etienne, B. Chaudret, *J. Mol. Catal. A Chem.* 212 (2004) 77.
- [109] M. Grellier, L. Vendier, B. Chaudret, A. Alberto, S. Rizzato, S. Mason, S. Sabo-Etienne, *J. Am. Chem. Soc.* 127 (2005) 17592.
- [110] P.A. Maltby, M. Schlaf, M. Steinbeck, A.J. Lough, R.H. Morris, W.T. Klooster, T.F. Koetzle, R.C. Srivastava, *J. Am. Chem. Soc.* 118 (1996) 5396.
- [111] G. Jia, C.P. Lau, *Coord. Chem. Rev.* 190–192 (1999) 83.
- [112] T.A. Luther, D.M. Heinekey, *Inorg. Chem.* 37 (1998) 127.
- [113] R.H. Morris, R.J. Wittebort, *Mag. Res. Chem.* 35 (1997) 243.
- [114] D.M. Heinekey, J.K. Law, S.M. Schultz, *J. Am. Chem. Soc.* 123 (2001) 12728.
- [115] G.J. Kubas, *Proc. Natl. Acad. Sci. U S A* 104 (2007) 6901.
- [116] J. Huhmann-Vincent, B.L. Scott, G.J. Kubas, *J. Am. Chem. Soc.* 120 (1998) 6808.
- [117] R.H. Morris, *Can. J. Chem.* 74 (1996) 1907.
- [118] G.J. Kubas, *Chem. Rev.* 107 (2007) 4152.
- [119] G. Jia, R.H. Morris, *J. Am. Chem. Soc.* 113 (1991) 875.
- [120] B.E. Douglas, D.H. McDaniel, J.J. Alexander, *Concepts and models of inorganic chemistry*, 3rd Ed. John Wiley & Sons, New York, 1994.
- [121] D.H. Lee, B.P. Patel, E. Clot, O. Eisenstein, R.H. Crabtree, *Chem. Commun.* (1999) 297.
- [122] C. Bianchini, C. Mealli, A. Sabat, *Inorg. Chem.* 25 (1986) 4617.
- [123] A.D. Wilson, A. Shoemaker, J.T. Miedner, J.T. Muckerman, D.L. DuBois, M.R. DuBois, *Proc. Natl. Acad. Sci. U S A* 104 (2007) 6951.
- [124] R.M. Bullock, B.J. Rappoli, *J. Chem. Soc. Chem. Commun.* (1989) 1447.
- [125] C.M. Nagaraja, M. Nethaji, B.R. Jagirdar, *Inorg. Chem.* 44 (2005) 4145.

- [127] M.S. Chinn, D.M. Heinekey, *J. Am. Chem. Soc.* 109 (1987) 5865.
- [128] F.A. Jalon, B.R. Moreno, A. Caballero, M.C. Carrion, L. Santos, G. Epsino, M. Moreno, *J. Am. Chem. Soc.* 127 (2005) 15364.
- [129] M. Schlaf, A.J. Laough, R.H. Morris, *Organometallics* 15 (1996) 4423.
- [130] V.K. Dioumaev, R.M. Bullock, *Nature* 424 (2000) 530.
- [131] M. Schlaf, P. Ghosh, P.J. Fagan, R.M. Bullock, *Angew. Chem. Int. Ed. Engl.* 40 (2001) 3887.
- [132] K. Abdur-Rashid, M. Faatz, A.J. Lough, R.H. Morris, *J. Am. Chem. Soc.* 123 (2001) 7473.
- [133] A. Volbeda, J.C. Fonticella-Camps, *Coord. Chem. Rev.* (2005) 1609.
- [134] M. Breyse, E. Furimsky, S. Kasztelan, M. Lacroix, G. Perot, *Catal. Rev.* 44 (2002) 651.
- [135] M. Neurock, R.A. van Santen, *J. Am. Chem. Soc.* 116 (1994) 4427.
- [136] S.P. Nolan, T.J. Marks, *J. Am. Chem. Soc.* 111 (1989) 8538.
- [137] M.T. Haward, M.W. George, P. Hamley, M. Poliakoff, *J. Chem. Soc. Chem. Commun.* 13 (1991) 913.
- [138] J. Eckert, G.J. Kubas, *Inorg. Chem.* 31 (1992) 1550.
- [139] G.J. Kubas, C.J. Burns, J. Eckert, S.W. Johnson, A.C. Larson, P.J. Vergamini, C.J. Unkefer, G.R.K. Khalsa, S.A. Jackson, O. Eisenstein, *J. Am. Chem. Soc.* 115 (1993) 569.
- [140] X.L. Luo, G.J. Kubas, C.J. Burns, J. Eckert, *Inorg. Chem.* 33 (1994) 5219.
- [141] T.M. Cameron, C.G. Ortiz, I. Ghiviriga, K.A. Abboud, J.M. Boncella, *J. Am. Chem. Soc.* 124 (2002) 922.
- [142] W.A. King, B.L. Scott, J. Eckert, G.J. Kubas, *Inorg. Chem.* 38 (1999) 1069.
- [143] A.K. Burrell, J.C. Bryan, G.J. Kubas, *J. Am. Chem. Soc.* 116 (1994) 1575.
- [144] D.M. Heinekey, C.E. Radzewich, M.H. Voges, B.M. Schomber, *J. Am. Chem. Soc.* 119 (1997) 4172.
- [145] V. Bakhmutov, T. Bürgi, P. Burger, U. Ruppli, H. Berke, *Organometallics* 13 (1994) 4203.
- [146] D. Woska, A. Prock, W.P. Giering, *Organometallics* 19 (2000) 4629.
- [147] J.S. Ricci, T.F. Koetzle, M.T. Bautista, T.M. Hofstede, R.H. Morris, J.F. Sawyer, *J. Am. Chem. Soc.* 111 (1989) 8823.
- [148] E.P. Cappellani, S.D. Drouin, G. Jia, P.A. Maltby, R.H. Morris, C.T. Schweitzer, *J. Am. Chem. Soc.* 116 (1994) 3375.
- [149] B. Chin, A.J. Lough, R.H. Morris, C.T. Schweitzer, C. D'Agostino, *Inorg. Chem.* 33 (1994) 6278.
- [150] M.J. Tenorio, M.C. Puerta, P. Valerga, *J. Chem. Soc. Chem. Commun.* (1993) 1750.
- [151] K.A. Leñero, M. Kranenburg, Y. Guari, P.C.J. Kamer, P.W.N.M. vanLeeuwen, S. Sabo-Etienne, B. Chaudret, *Inorg. Chem.* 42 (2003) 2859.
- [152] T.P. Fong, A.J. Lough, R.H. Morris, A. Mezzetti, E. Rocchini, P. Rigo, *J. Chem. Soc. Dalton Trans.* (1998) 2111.
- [153] M.S. Chinn, D.M. Heinekey, *J. Am. Chem. Soc.* 109 (1987) 5865.
- [154] C.A. Tolman, *Chem. Rev.* 77 (1977) 313.
- [155] N. Mathew, B.R. Jagirdar, R. Srinivasa, G.U. Kulkarni, *Organometallics* 19 (2000) 4506.
- [156] N. Mathew, B.R. Jagirdar, *Inorg. Chem.* 39 (2000) 5404.
- [157] N. Mathew, B.R. Jagirdar, A. Ranganathan, *Inorg. Chem.* 42 (2003) 187.
- [158] M. Kranenburg, P.C.J. Kamer, W.N.M. van Leeuwen, B. Chaudret, *Chem. Commun.* (1997) 37.
- [159] C. Bianchini, C. Mealli, A. Meli, M. Peruzzini, F. Zanobini, *J. Am. Chem. Soc.* 110 (1988) 8725.
- [160] C. Bianchini, C. Mealli, M. Peruzzini, F. Zanobini, *J. Am. Chem. Soc.* 109 (1987) 5548.
- [161] D.M. Heinekey, A. Leigeois, M. vanRoon, *J. Am. Chem. Soc.* 116 (1994) 8388.
- [162] M.J. Ingleson, S.K. Brayshaw, M.F. Mahon, G.D. Ruggiero, A.S. Weller, *Inorg. Chem.* 44 (2005) 3162.
- [163] V.I. Bakhmutov, C. Bianchini, M. Peruzzini, F. Vizza, E.V. Vorontsov, *Inorg. Chem.* 39 (2000) 1655.
- [164] W.P. Anderson, T.R. Cundari, R.S. Drago, M.C. Zerner, *Inorg. Chem.* 29 (1990) 3.
- [165] C. Bianchini, S. Moneti, M. Peruzzini, F. Vizza, *Inorg. Chem.* 36 (1997) 5818.
- [166] G.A. Ozin, J. Garcia-Prieto, *J. Am. Chem. Soc.* 108 (1986) 3099.
- [167] B.F.M. Kimmich, R.M. Bullock, *Organometallics* 21 (2002) 1504.
- [168] M.D. Butts, B.L. Scott, G.J. Kubas, *J. Am. Chem. Soc.* 118 (1996) 11831.
- [169] B. Pleune, D. Morales, R. Meunier-Prest, P. Richard, E. Collange, J.C. Fettingier, R. Poli, *J. Am. Chem. Soc.* 121 (1999) 2209.
- [170] M. Baya, J. Houghton, J.C. Daran, R. Poli, *Angew. Chem. Int. Ed. Engl.* 46 (2007) 429.
- [171] M. Baya, J. Houghton, J.C. Daran, R. Poli, L. Male, A. Albinati, M. Gutman, *Chem. Eur. J.* 13 (2007) 5347.
- [172] Dedicated website of the US Department of Energy, at: <http://www.hydrogen.energy.gov/storage.html>.
- [173] H. Arakawa, M. Aresta, J. Armor, M. Barteau, E. Beckman, A. Bell, J. Bercaw, C. Creutz, D.A. Dixon, D. Dixon, *Chem. Rev.* 101 (2001) 953.
- [174] S.K. Brayshaw, J.C. Green, N. Hazari, J.S. McIndoe, F. Marken, P.R. Raithby, A.S. Weller, *Angew. Chem. Int. Ed. Engl.* 45 (2006) 6005.
- [175] A. Zecchina, S. Borgida, J. Vitillo, G. Ricchiardi, C. Lamberti, G. Spoto, M. Bjørgen, K.P. Lillerud, *J. Am. Chem. Soc.* 127 (2005) 6361.
- [176] J.L.C. Rowsell, E.C. Spencer, J. Eckert, J.A.K. Howard, O.M. Yaghi, *Science* 309 (2005) 1350.
- [177] J. Hélarý, N. Salandre, J. Sailard, D. Poullain, A. Beaucamp, D. Autissier, *Int. J. Hydrog. Energ.* 34 (2009) 169.
- [178] W. Grochala, P.P. Edwards, *Chem. Rev.* 104 (2004) 1283.
- [179] T.M. Douglas, S.K. Brayshaw, R. Dallanegra, G. Kociok-Köhn, S.A. Macgregor, G.L. Moxham, A.S. Welle, P. Wondimagegn, *Vadivelu, Chem. Eur. J.* 14 (2008) 1004.
- [180] R.D. Adams, B. Captain, *Acc. Chem. Res.* 42 (2009) 409.
- [181] S.K. Brayshaw, M.J. Ingleson, J.C. Green, J.S. McIndoe, P.R. Raithby, G. Kociok-Köhn, A.S. Weller, *J. Am. Chem. Soc.* 128 (2006) 6247.
- [182] S.K. Brayshaw, M.J. Ingleson, J.C. Green, P.R. Raithby, G. Kociok-Köhn, J.S. McIndoe, A.S. Weller, *Angew. Chem. Int. Ed. Engl.* 44 (2005) 6875.
- [183] M.J. Ingleson, M.F. Mahon, P.R. Raithby, A.S. Weller, *J. Am. Chem. Soc.* 126 (2004) 4784.
- [184] R.D. Adams, B. Captain, D.M. Smith, *Angew. Chem. Int. Ed. Engl.* 45 (2006) 1109.
- [185] A.J. Esswein, D.G. Nocera, *Chem. Rev.* 44 (2007) 4022.
- [186] A.V. Levina, A. Rossin, N.V. Belkova, M.R. Chierotti, L.M. Epstein, O.A. Filippov, R. Gobetto, L. Gonsalvi, A. Lledós, E.S. Shubina, F. Zanobini, M. Peruzzini, *Angew. Chem. Int. Ed. Engl.* 50 (2011) 1367.
- [187] N.V. Belkova, L.M. Edstein, E.S. Shubina, *Eur. J. Inorg. Chem.* (2010) 3555.
- [188] P.A. Dub, M. Baya, J. Houghton, N.V. Belkova, J.C. Daran, R. Poli, L.M. Epstein, E.S. Shubina, *Eur. J. Inorg. Chem.* (2007) 2813.
- [189] S.L. Matthews, D.M. Heinekey, *J. Am. Chem. Soc.* 118 (2006) 2615.
- [190] P.M. Vignais, B. Billoud, *Chem. Rev.* 107 (2007) 4206.
- [191] W. Lubitz, E. Reijerse, J. Messinger, *Energy Environ. Sci.* 1 (2008) 15.
- [192] M.W.W. Adams, E.I. Stiefel, *Science* 282 (1998) 1842.
- [193] R. Cammack, *Nature* 397 (1999) 214.
- [194] D.G. Nocera, *Chem. Soc. Rev.* 38 (2009) 13.
- [195] A.J. Esswein, D.G. Nocera, *Chem. Rev.* 107 (2007) 4022.
- [196] N.S. Lewis, D.G. Nocera, *Proc. Natl. Acad. Sci. U S A* 103 (2006) 15729.
- [197] J.C. Gordon, G.J. Kubas, *Organometallics* 29 (2010) 4682.
- [198] A. LeGoff, V. Artero, B. Joussemle, P. Dinh Tran, N. Guillet, R. Metaye, A. Fihri, S. Palacin, M. Fontecave, *Science* 326 (2009) 1384.
- [199] A. Fihri, V. Artero, M. Razavet, C. Baffert, W. Leibl, M. Fontecave, *Angew. Chem. Int. Ed. Engl.* 47 (2008) 564.
- [200] L. Sun, B. Akermark, S. Ott, *Coord. Chem. Rev.* 249 (2005) 1653.
- [201] R. Lomoth, S. Ott, *Dalton Trans.* (2009) 9952.
- [202] W.G. Wang, F. Wang, H.Y. Wang, G. Si, C.H. Tung, L.Z. Wu, *Chem. Asian J.* 5 (2010) 1796.